Quaternary Science Reviews 392 (2026) 110288

Contents lists available at ScienceDirect

Quaternary Science Reviews

journal homepage: www.elsevier.com/locate/quascirev

Contextualising early hominin environments: A multi-proxy palaeoenvironmental reconstruction of the earliest Oldowan at Nyayanga, western Kenya

Thomas Vincent [a,1], Timothy Lane [b,*,1], Elizabeth Whitfield [a], Peter Ditchfield [c], Rahab N. Kinyanjui [d,e,f], Scott A. Blumenthal [f,g,h], Emma M. Finestone [i], James Oliver [j], Laura C. Bishop [k], Jensen Wainwright [g], Blasto Onyango [d], Richard Potts [d,f], Thomas Plummer [f,l,m,n]

[a] School of Biological and Environmental Sciences, Liverpool John Moores University, Byrom Street, Liverpool, L3 3AF, United Kingdom
[b] Department of Geoscience, and iClimate, Aarhus University, Aarhus, 8000, Denmark
[c] School of Archaeology, University of Oxford, 1 South Parks Rd, Oxford, OX1 3TG, United Kingdom
[d] Earth Science Department, National Museums of Kenya, P.O Box 40658-00100, Nairobi, Kenya
[e] Department of Archaeology, Max Planck Institute for Geoanthropology, Kahlaische Straße 10, Jena, 07745, Germany
[f] Human Origins Program, National Museum of Natural History, Smithsonian Institution, P.O. Box 37012, Washington, DC, 20560, USA
[g] Department of Anthropology, University of Oregon, 1585 East 13th Avenue, Eugene, OR, 97403, USA
[h] Department of Earth, Ocean and Atmospheric Sciences, University of British Columbia, Vancouver, BC, V6T 1Z4, Canada
[i] Department of Anthropology, Cleveland Museum of Natural History, 1 Wade Oval Dr, Cleveland, OH, 44113, USA
[j] Anthropology Section, Illinois State Museum - RCC, Springfield, IL, 62706, USA
[k] The Sino-British College, University of Shanghai for Science and Technology, 1195 Middle Fuxing Rd, Shanghai, 200031, PR China
[l] Department of Anthropology, Queens College, 65-30 Kissena Boulevard Flushing, Flushing, NY, 11367, USA
[m] New York Consortium in Evolutionary Primatology, New York, NY, USA
[n] The CUNY Graduate Center, 365 5th Ave, New York, NY, 10016, USA

ARTICLE INFO

Handling Editor: Dr Mira Matthews

Keywords:
Oldowan
Palaeoenvironmental reconstruction
Sedimentology
Phytolith
Stable isotopes

ABSTRACT

Several early Oldowan localities are known from the Homa Peninsula, in southwestern Kenya, the oldest of which, Nyayanga (~3–2.6 Ma), preserves the earliest known evidence of Oldowan tool assemblages, long-distance raw material transport, and butchery. Here, we present a multi-proxy reconstruction of hominin environments at Nyayanga, using stratigraphy, particle size, phytoliths, and stable isotopes to reconstruct the site's sedimentary dynamics, depositional environment, and palaeovegetation. Four units have been identified from Nyayanga (NY-1 to NY-4); this study concentrates on NY-1 to NY-3. The site is interpreted as a former alluvial plain environment where deposition occurred through episodic hyperconcentrated flows and intermittent unconfined fluvial flows. During flow hiatus, secondary processes, including fluvial runoff and aeolian deposition, occurred, along with the development of a stable land surface. Climatic conditions at Nyayanga are characterized as moderately seasonal and well-watered. Isotopic analyses of fossil mammals and pedogenic carbonates, alongside phytolith taxonomic analyses, demonstrate that C_3 vegetation is underrepresented throughout the sequence, whereas higher abundances of C_4 plants could indicate a dense ground cover. Based on multi-proxy evidence, the landscape at Nyayanga becomes more stable through time, showing less frequent higher-energy, hyperconcentrated flows and less unconfined fluvial activity. Soil development increases and becomes more mature with varying levels of pedogenesis.

* Corresponding author.
E-mail address: timothy.lane@geo.au.dk (T. Lane).
[1] These authors contributed equally to this work.

https://doi.org/10.1016/j.quascirev.2026.110288
Received 4 February 2026; Received in revised form 15 September 2026; Accepted 16 September 2026
Available online 22 September 2026
0277-3791/Crown Copyright © 2026 Published by Elsevier Ltd. This is an open access article under the CC BY license (http://creativecommons.org/licenses/by/4.0/).

1. Introduction

Understanding the environmental contexts associated with early hominin evolution is a key research focus in palaeoanthropology (Cohen et al., 2022). Lomekwian stone tools from 3.3 Ma represent the earliest known stone tools (Harmand et al., 2015), and are characterised by core-and-flake technology, with large cores, flakes, and anvils (see Plummer et al., 2025 for a summary). However, the appearance of Oldowan hominin technology around 2.6 - 2.9 million years ago (Ma) marked a crucial behavioural innovation and evolutionary milestone (Semaw et al., 1997; Braun, 2009; Plummer et al., 2023; Toth and Schick, 2018; Braun et al., 2019, 2025). This change in toolmaking proficiency was characterised by selectivity in raw material use, and expert knapping technique, and associated with large mammal butchery, dietary changes, and transport of raw materials for lithic production. Research has focused on testing hypotheses relating hominin evolution and behavioural changes (such as the emergence of Oldowan technology), to changes in climate or environment (Vrba, 1985; Potts, 1994; Albert et al., 2015; Plummer et al., 1999). The Oldowan industry is found in association with eastern African landscapes increasingly dominated by C_4 vegetation (grasses and sedges) and grazing mammals, with these ecological changes potentially driven by regional drying, cooling, tectonic uplift, shifts in rainfall seasonality, and/or fire (Plummer and Bishop, 1994; Behrensmeyer et al., 1997; Uno et al., 2016a, 2016b; Blumenthal et al., 2017; Braun et al., 2025). Recent studies have also highlighted the importance of high-amplitude oscillations in vegetation composition correlated with precipitation changes, suggesting that orbital-scale variation in precipitation may represent an important driver of vegetation change (Lupien et al., 2021). Empirical and modelling studies indicate that hominins inhabited mosaic, often unstable environments during this period that may have no modern analogues, highlighting the need to directly reconstruct past ecosystem change and their underlying drivers (Lupien et al., 2021; Patterson et al., 2017; Zeller et al., 2023; Faith et al., 2019). However, terrestrial palaeoenvironmental reconstructions from hominin sites in eastern Africa within the 2.6 - 3.0 Ma period are scarce and often rely on reconstructions from more distant boreholes sampling lake sediments, or indirect evidence such as taxonomic or dietary information from large mammal fauna (Plummer et al., 2023; Braun et al., 2025). Isotopic studies of pedogenic carbonates provide detailed records of shifts in the abundance of C_3 and C_4 vegetation but often are not collected in direct association with hominin fossils or stone tools and are predominately from the Omo-Turkana, Awash, and Baringo Basins (Cerling et al., 2011, 2013; Levin et al., 2011; Patterson et al., 2017; Plummer et al., 2009).

A key challenge of palaeoanthropology is to demonstrate how hominin behaviours are related to environmental variability. Multiproxy approaches utilising various palaeoenvironmental reconstructive techniques provide powerful means to address changes in plant and animal communities relevant to hominins at local to regional scales. Given that proxies reflect different aspects of the environment, multiproxy studies are able to help provide nuance to often unclear environmental signals. This increases confidence in environmental reconstructions and provides clarity to better understand environmental change. These studies help to provide invaluable context for hominin behaviour and allow site-based environmental reconstructions (Albert et al., 2015; Bamford et al., 2006; Mercader et al., 2021; Braun et al., 2025; Potts et al., 2018).

In this study, we use sedimentology, phytolith analysis, and isotopic analysis to investigate past sedimentary dynamics, depositional environments, vegetation, and climatic conditions through the sedimentary sequence at the late Pliocene hominin site Nyayanga, western Kenya (Plummer et al., 2023). Thus, it aims to elucidate the drivers of palaeoenvironmental change during a critical window of hominin evolution in a less-studied region of eastern Africa.

2. Setting

The Homa Peninsula in southwestern Kenya lies on the southern shores of the Winam Gulf of Lake Victoria in the Nyanza Rift, an elongate EW to NE–SW fault-bounded rift system which emanates from the Kenya dome (Pickford, 1982; Behrensmeyer et al., 1995; Bishop et al., 2006; Ditchfield et al., 1999; Plummer et al., 1999). East of Lake Victoria, the rift is 133 km long, with a width of 25 – 50 km (Behrensmeyer et al., 1995). The peninsula is dominated by the Homa Mountain carbonatite complex, which is formed from predominantly intrusive igneous lithologies emplaced on a basement of shattered and fenitized Nyanzian rocks. Doming of Homa Mountain began at ~10 –11 Ma and continued until around 5 Ma, with the latest dated episode occurring at 1.3 ± 0.1 Ma (Behrensmeyer et al., 1995). The geology near Homa Mountain includes Homa Mountain carbonatite complex, various phonolite intrusions and lavas, various pyroclastic deposits, and fenitized Nyanzian andesite and rhyolite (Braun et al., 2008; Finestone et al., 2025; Saggerson, 1952). From 6 Ma, fluvial, alluvial, and lacustrine deposits have accumulated around the margin of Homa mountain (Behrensmeyer et al., 1995; Braun et al., 2008; Ditchfield et al., 1999; Plummer et al., 1999). Extensive geological mapping, geochemical analyses, and conglomerate surveys have revealed that past and modern drainages across the peninsula predominantly deposit material from the carbonatite complex, indicating that this is the primary sediment source (Braun et al., 2008; Finestone et al., 2025). At the present day, the Homa Peninsula's annual average precipitation is 1400 mm, and its average temperature is 24^0C (Le Bas, 1977). Although classified as a tropical climate, rainfall in the region is erratic and prolonged droughts are common. The complex topography of this region results in a highly diverse set of mean rainfall totals, with highlands receiving 1500 mm of mean annual rainfall, and lowlands receiving 250 – 500 mm. Regionally, the mountain ranges surrounding the central rift valley also act as an orographic barrier producing a rain shadow effect that results in irregular rainfall throughout the long rainy season between March and May (MUTAI and WARD, 2000{Kinyanjui, 2012 #33)}.

The Homa Peninsula preserves several important localities (Fig. 1), including Kanam (Kent, 1942), Sare-Abururu (Finestone et al., 2024), Kanjera (Oliver et al., 2019; Plummer et al., 1999; Ferraro et al., 2013), and the focus of this study, Nyayanga (Plummer et al., 2023).

Nyayanga (0° 23′ 55.597″ S, 34° 27' 5.767" E) lies west of Homa Mountain, on the western shoreline of the Homa Peninsula (Fig. 1). Its landscape is characterised by extensive faulting, and fluvial incision into clays, silts, and sands, which have shaped a 40,000 m^2 westward facing amphitheatre, where well-stratified beds can be observed in a ~16 m thick sequence (Fig. 1). Elevation steeply decreases from east to west here, with Homa Mountain acting as the only fluvial sediment source for the sites. Today, the vegetation consists of an open wooded grassland, with shrubs and grasses being common, and much of the surrounding land under cultivation.

The broad lithostratigraphic sequence at Nyayanga is described in Plummer et al. (2023) and outlined below. The lowest exposed unit is a thick (>10 m) sequence of interbedded sandstones and weakly cemented conglomeratic layers, which belong to the Homa Formation (Pickford, 1984). These underlying Homa Formation deposits have a biostratigraphic age of ca. 4.0 - 3.5 Ma (Bishop et al., 2022) and are not discussed further here. The oldest Nyayanga Bed (NY-1) lies unconformably above the Homa Formation, and is characterised by a strongly erosive base, and a fining upward channel sequence. NY-2 is characterised by orange clayey silts with frequent pedogenic alteration, likely deposited as overbank deposits of the fluvial system which deposited NY-1. NY-3 overlies NY-2 with a weakly erosive contact, and is composed of clayey silts, with high concentrations of coalescing carbonate nodules, representing terrestrial deposition with periods of landscape stability. NY-4 has an erosive contact with NY-3, and displays a poorly sorted, fining upwards sequence.

Tools found at Nyayanga have extended the geographic distribution

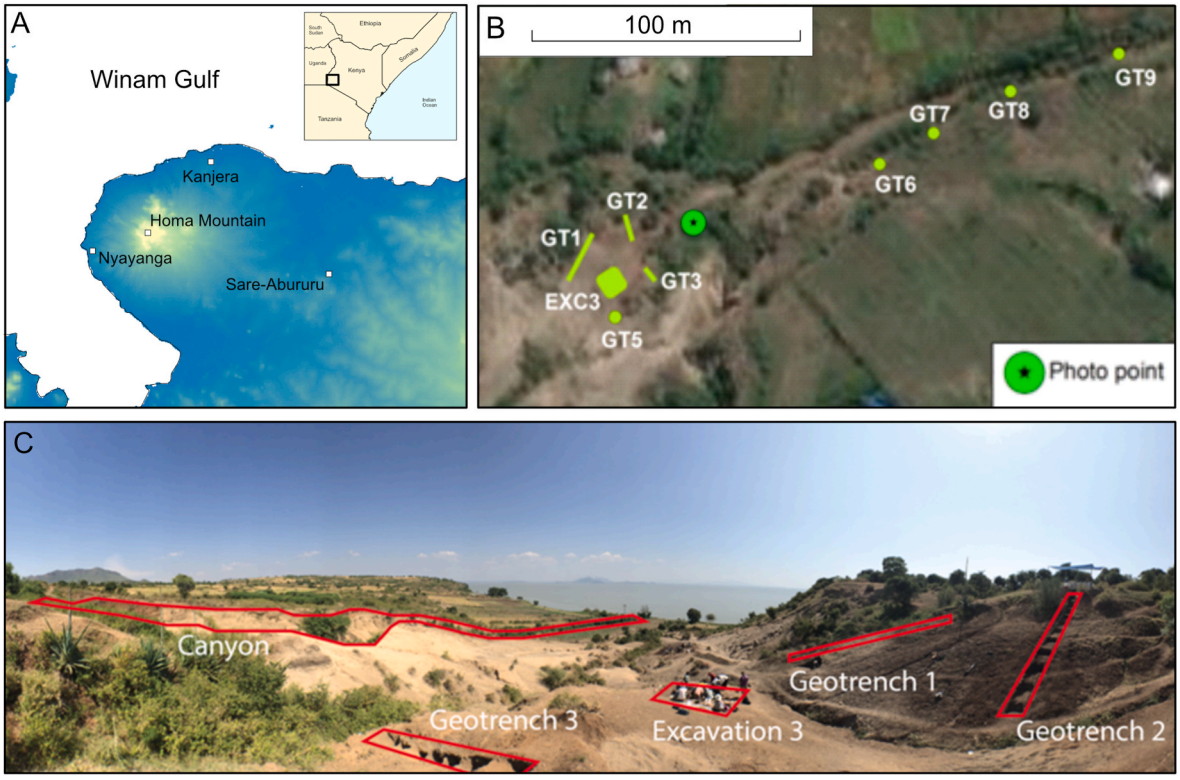


Fig. 1. (A) Location map showing the Homa Peninsula, in the Winam Gulf of Lake Victoria, the study site (Nyayanga), and other sites mentioned in the text. (B) Aerial photograph of the Geological trenches (GT) and excavations (EXC) at Nyayanga. (C) A ~ 150 m panoramic site photograph taken from the photo point displayed in Fig. 1 facing southwest (0°23′54.38"S, 34°27′8.27′ E). Geological trenches and excavations placed in the main amphitheatre of the Nyayanga locality are labelled in the figure. Geological trenches placed further up the canyon are not visible in Fig. 1C.

of the earliest Oldowan archaeological industry by over 1300 km (Plummer et al., 2023). During fieldwork at the locality, six excavations and over twenty geological trenches were dug, with Oldowan artifacts documented in the Nyayanga Beds (NY-1 to NY-4). At present, 401 artifacts have been discovered from unit NY-1, of which 129 were found *in situ* in excavations (Finestone et al., 2025). Artifacts were also found *in situ* in Beds NY-2, NY-3 and NY-4 and are currently under analysis. Two hippopotamid butchery sites were documented in NY-1, and stone tool cut marks, percussion damage, and use-wear indicate that hominins were processing both plant and animal tissue (Plummer et al., 2023). *Paranthropus* molars from two different individuals were also recovered from NY-1, suggesting Paranthropus may have been the hominin using Oldowan tools to process plants and animals at Nyayanga. The chronology of unit NY-1, based on biostratigraphy, (U-Th)/He apatite crystal ages, and magnetostratigraphy, places the deposits associated with Oldowan technology at 3.050 – 2.595 Ma in age (Plummer et al., 2023), demonstrating that the Oldowan is older than previously thought. Initial palaeoenvironmental investigation reported that these behaviours occurred in a relatively open, grass-rich environment (Bishop et al., 2006; Ditchfield et al., 1999; Plummer et al., 1999, 2023; Plummer and Bishop, 2016). Nyayanga, therefore, represents a unique and valuable record of early Oldowan activity and an important opportunity to better understand the environmental settings in which hominins used these tools (Plummer et al., 2009; Potts, 2012). This study focuses on beds NY-1, NY-2, and NY-3, to investigate the palaeoenvironmental conditions of this period of Oldowan habitation.

3. Methods

3.1. Field investigation

A total of 206 sediment spot samples were taken from units NY-1 to NY-3 throughout eight geological trenches (Fig. 4, GT1 n = 37, GT2 n = 33, GT3 n = 34, GT5 n = 13, GT6 n = 24, GT7 n = 18, GT8 n = 27, GT9 n = 20). Samples of 100-300g of sediment were taken throughout exposed sediment sections, to ensure enough sediment for all analysis and capture sedimentological variation. Before taking samples, the weathering profile was scraped off the face of the sequence with a stainless-steel trowel. After removal, a hand lens was used to inspect carbonate nodules, and any coalescing carbonates and carbonate horizons were noted. The classification system proposed by Miall (2013) was used to provide a basis for identifying lithofacies across all trenches and to adhere to a standardised classification system. Samples were taken from each lithofacies and at laterally varying, stratigraphically equivalent locations. Observations were made on colour, composition, sedimentary structures and particle size class(es). A more detailed and laterally extensive architectural analysis was not possible because sediment exposures were limited to geological trenches and excavations (Miall, 2013). Throughout the study, care was taken to ensure stratigraphic equivalence when sampling in a highly faulted local environment. Broader conglomeratic surveys identifying geological provenances surrounding the sites have previously been completed (Finestone et al., 2025) and were not undertaken here.

3.2. Particle size analysis

Whilst geological provenances and sediment sources surrounding Nyayanga have been identified in previous studies (Braun et al., 2008; Finestone et al., 2025; Plummer et al., 2023), little is known about past transport and depositional mechanisms at these sites. Particle size analysis (PSA) was completed on all 206 sediment samples to characterise the fine particle size fraction (<2 mm). Samples were subject to chemical pre-treatment similar to that outlined by Konert and Vandenberghe (1997) to provide an evenly dispersed suspension (Liu

et al., 2014). 10 ml of 30% H_2O_2 was added to oxidise samples and remove unwanted organic material that might reduce the repeatability of results or skew particle size distributions (Blott et al., 2004; Gray et al., 2010). Subsequently, samples were heated for further oxidation until all reactions ceased. Carbonates, including those derived from the Homa mountain carbonatite complex, were not removed by hydrochloric acid, as these were suspected to make up a large proportion of the samples and be part of the original depositional medium. Samples were then placed in a 40^0C oven until almost all the water had evaporated. Sodium hexametaphosphate was added to ensure the even dispersal of particles. A Beckman Coulter LS11320 laser granulometer was used to measure particle size using the Fraunhofer model, as the samples contained coarser material (>63 μm). Analyses of samples were repeated five times to ensure reproducibility. GRADISTAT was used to calculate textural parameters and size classes in the phi unit using the Folk and Ward method (Folk and Ward, 1957).

3.3. End-member mixing analysis

End-member mixing analysis (EMMA) is the process of decomposing or 'unmixing' particle size distributions into constituent components or end-members (EMs). EMs provide more meaningful interpretations of sediment dynamics from particle size distributions and often represent the sediment pool, pathway, or mixing dynamics of the environment (Weltje, 1997; Weltje and Prins, 2003, 2007; Meyer et al., 2013; Paterson and Heslop, 2015; van der Bilt et al., 2021). EMMA has been utilised in various sedimentary archives to identify sediment sources and/or transport mechanisms (Dietze and Dietze, 2019). AnalySize, the EMMA interface developed within MATLAB, was used to calculate non-parametric EMs for the datasets (Paterson and Heslop, 2015).

3.4. Phytoliths

Sediment was prepared for phytolith analysis using the method described by Bamford et al. (2006) and Albert et al. We prepared a total of 68 samples for phytolith analysis (Fig. 4, GT1 n = 17, GT2 n = 13, GT3 n = 11, GT5 n = 4, GT6 n = 7, GT7 n = 4, GT8 n = 7, GT9 n = 5). Samples were treated with 10% Hydrochloric acid to eliminate carbonates and phosphates, and 10% Nitric acid to eliminate organic matter. Each acid treatment was followed by two washes with distilled water; samples were centrifuged at 3000 r.p.m. for 2 min and decanted between washes. The samples were also treated with hydrogen peroxide to further remove more labile organic matter through oxidation. The acid-insoluble fraction was then subject to density separation by adding a sodium polytungstate solution of 2.4 g/ml density (Albert et al., 2006, 2015; Albert and Weiner, 2001).

Broadly, phytolith identification and classification followed International Codes for Phytolith Nomenclature (ICPN) 1.0 and 2.0 (Madella et al., 2005; Neumann et al., 2019) as well as classifications of numerous published sources (Twiss et al., 1969; Brown, 1984; Piperno, 2006, 2014; Piperno and Pearsall, 1998; Albert et al., 2016), the PHYTCORE online database (http://www.phytcore.org), and the modern reference collection housed at the National Museums of Kenya, described in Kinyanjui (2012). A minimum of 200 phytoliths with recognisable morphologies was counted to ensure a maximum 24% error margin in interpreting results (Bamford et al., 2006). Phytoliths are broadly categorised based on the type of vegetation taxa in which they occur in abundance: grasses, sedges, trees & shrubs, and a generalist/non-diagnostic category. Phytoliths produced in abundance by a particular vegetation group but also made in different plants are categorised as "generalist/non-diagnostic". Morphotypes identified in the phytolith assemblage were counted and presented for each sampling location. Phytoliths for each category were displayed as a percentage of the total count, plotted against the depth of the geological trench. Changes in the percentages of these groups are considered to reflect changes in the structure of the palaeovegetation (Piperno, 2006; Kinyanjui, 2012).

3.5. Isotopic analysis

For comparison with sedimentological and phytolith data, we have synthesised previously published isotopic studies of palaeosol carbonates and mammalian tooth enamel (Plummer et al., 2023) and present revised estimates of woody cover and isotopic seasonality of precipitation.

3.5.1. Pedogenic carbonates and woody cover

The carbon isotope composition ($\delta^{13}C$) of palaeosol organic matter and pedogenic carbonates reflects the isotopic composition of overlying vegetation during formation (Cerling, 1984), and is widely used to investigate environmental change in Africa (Sikes, 1994; Plummer et al., 2009; Finestone et al., 2024; Potts et al., 1999; Levin et al., 2011). Pedogenic carbonate $\delta^{13}C$ can be used to quantify the fraction of C_3 plant matter, which can be used to distinguish vegetation structure categories: grasslands (0-10% woody cover), open wooded grasslands (10-20%), wooded grasslands (20-40%), grassy woodlands/bushlands/shrublands (40-60%), woodlands/bushlands/shrublands (60-80%), and forests (80-100%) (Cerling et al., 2011, 2013). As described by Plummer et al. (2023), pedogenic carbonates at Nyayanga were collected from palaeosol horizons exposed in paleomagnetism trench 01. Each nodule was collected from >30 cm in depth from the top of each horizon such that their carbon isotope composition reflects plant-derived soil CO_2 rather than ^{13}C-enriched atmospheric CO_2 (Cerling et al., 1989). To exclude non-pedogenic carbonates, we analysed only small (diameter < 1.5 cm), micritic nodules with rhizolith morphologies such as vertical, tubular, downward branching forms. Only nodules that showed no signs of recrystallisation in the form of internal or external, sparry, calcite cements were selected for analysis. We also exclude carbonates from horizons containing apparently transported, rounded carbonate nodules, as well as large or diffuse nodules. Pedogenic carbonate nodules typically form over 10^2-10^5 years, but small nodules (<2 cm diameter) such as those collected from Nyayanga likely form in <5000 years (Retallack, 2005), during periods of relative landscape stability and pedogenic development. Finally, samples were cleaned of any adhering sediment prior to analysis.

The carbon isotope composition of carbonate nodules collected from a temporary geotrench close to Excavations 3 and 5, used for palaeomag and pedogenic isotope sampling. Samples were taken from NY-1 (n = 2), NY-2 (n = 2), and NY-3 (n = 1) in order to estimate woody cover using a widely used global model relating soil $\delta^{13}C$ to woody cover (Cerling et al., 2011; Plummer et al., 2023). In this study, we revise palaeo-woody cover estimates for Nyayanga pedogenic carbonates using a region-specific model, the Eastern Africa woody cover model (EAWCM), which was developed using a significantly expanded dataset of soil $\delta^{13}C$ compared to the original global model, as well as revised remote sensing-based woody cover estimates for each modern soil sampling location (Negash et al., 2024). Following the EAWCM, the fraction of woody cover is estimated from the carbon isotope composition of a palaeosol sample using the following relationship:

$$Fwc = \left(\sin\left[-0.957851 - 0.086563 \times \delta^{13}C\right]\right)^2$$

The predicted probability density distribution of the fraction of woody cover is calculated using previously published MATLAB code (Cerling et al., 2011), updated with parameters from the EAWCM.

3.5.2. Equid teeth and palaeoseasonality

The oxygen isotope composition ($\delta^{18}O$) of mammalian bioapatite, such as tooth enamel, reflects the isotopic composition of an individual's body water (Longinelli, 1984; Bryant and Froelich, 1995; Kohn, 1996), and variations within teeth can reflect isotopic changes of local waters related to seasonality in precipitation amount or source during the

periods of enamel formation, or seasonal migration during enamel formation (Kohn et al., 1998; Fricke et al., 1998; Green et al., 2018; Blumenthal et al., 2019). Equids are especially useful targets for reconstructing aspects of precipitation seasonality because their hypsodont teeth grow over multiple years and, as water-dependent grazers, the oxygen isotope composition of their tooth enamel reflects local meteoric (rainfall-derived) waters (Bryant et al., 1994; Huertas et al., 1995; Hoppe, 2006; Blumenthal et al., 2017), and oxygen isotopic variability within teeth can be used to address past precipitation seasonality (Sharp and Cerling, 1998; Blumenthal et al., 2019; Norwood et al., 2025). Among eastern African zebra, the amplitude of isotopic variation within teeth provides a quantitative indicator of the amplitude of isotopic seasonality of precipitation, and even small sample sizes can provide an indication of broad shifts in past climate (Blumenthal et al., 2019). An initial estimate of palaeoseasonality at Nyayanga was based on intratooth $\delta^{18}O$ variation in a single *Eurygnathohippus* upper third molar from NY-1 (Plummer et al., 2023). In this study we report results from isotopic analysis of intratooth samples collected from two additional *Eurygnathohippus* molars from unit NY-1, including an upper molar (NY15-40) and lower molar (NY15-29). The new total sample of NY-1 equids ($n = 3$) is similar to, and in several cases greater than, the sample size of a given taxon from a given fossil assemblage in previous isotopic studies of Plio-Pleistocene fossil mammal teeth aimed at addressing paleoseasonality through intratooth sampling (Souron et al., 2012; Briatico et al., 2024; Uno et al., 2018).

The fossil equid specimens are housed at the National Museum of Kenya and were sampled at 3-5 mm intervals along the tooth growth axis using a diamond-tipped handheld rotary drill. To remove diagenetic secondary carbonates, the enamel powder was treated with 0.1 M buffered acetic acid for 15 min, rinsed three times to neutrality, and dried overnight at 60 °C. Before analysis, treated enamel powder was weighed into 4.5 mL Exetainer vials. Vials were opened and dried at 60 °C in an oven and transferred to a GasBench II carbonate device, where they were purged with helium. Samples were reacted with 104% phosphoric acid at 70 °C for 1 h. The carbon and oxygen isotope ratios of the resulting CO_2 were determined using a Thermo MAT 253 isotope ratio mass spectrometer housed in the University of Oregon Stable Isotope Laboratory. Results are reported in per mil (‰) notation, where $\delta^{13}C = (R_{sample}/R_{standard}\text{-}1) * 1000$, where R_{sample} and $R_{standard}$ are the $^{13}C/^{12}C$ ratios of the sample and standard, respectively. Fossil samples were analysed alongside standards used to assess instrumental drift and to normalise $\delta^{13}C$ and $\delta^{18}O$ measurements to the international Vienna Pee Dee Belemnite (V-PDB) scale. Standards used include B2214 carrara marble ($\delta^{13}C = 2.1 \pm 0.07‰$, $\delta^{18}O = -2.01 \pm 0.1‰$) and two in-house laboratory tooth enamel standards, including fossil bison enamel ($\delta^{13}C = -11.1 \pm 0.2‰$, $\delta^{18}O = -18.2 \pm 0.2‰$) and modern buffalo enamel ($\delta^{13}C = 0.2 \pm 0.1‰$, $\delta^{18}O = 3.03 \pm 0.2‰$). Tooth enamel $\delta^{18}O$ is corrected for temperature-dependent fractionation of carbonate to CO_2 ($\alpha_{70} = 1.0071$ for non-modern tooth enamel, $\alpha_{70} = 1.00848$ for modern tooth enamel, and $\alpha_{70} = 1.00949$ for calcite) (Kusaka and Nakano, 2014). Reproducibility is indicated by repeated $\delta^{13}C$ and $\delta^{18}O$ measurements of standards, which were 0.2‰ ($\pm 1\sigma$) or better.

The primary isotopic signature of tooth enamel is partially obscured due to enamel formation, mineralisation, and isotopic time averaging in the animal's body water pool (Passey and Cerling, 2002; Blumenthal et al., 2014). The intratooth $\delta^{18}O$ ranges from equid teeth can be corrected for this signal loss by application of a damping factor, calculated from comparing the actual amplitude of the environmental signal to the amplitude measured in the tooth profiles (Blumenthal et al., 2019). This signal can range from 0.0 (all original environmental signal retained) to 1.0 (all signal lost). We use a damping factor of 0.536, calculated based on the amplitude of modern precipitation and the amplitude of modern equid teeth from Kenya (Blumenthal et al., 2019). Following the relationship between modern equid intratooth $\delta^{18}O$ range and precipitation intra-annual $\delta^{18}O$ range, the intra-annual $\delta^{18}O$ range of precipitation in the fossil record can be estimated from corrected (i.e. undamped) intratooth $\delta^{18}O$ ranges.

4. Results

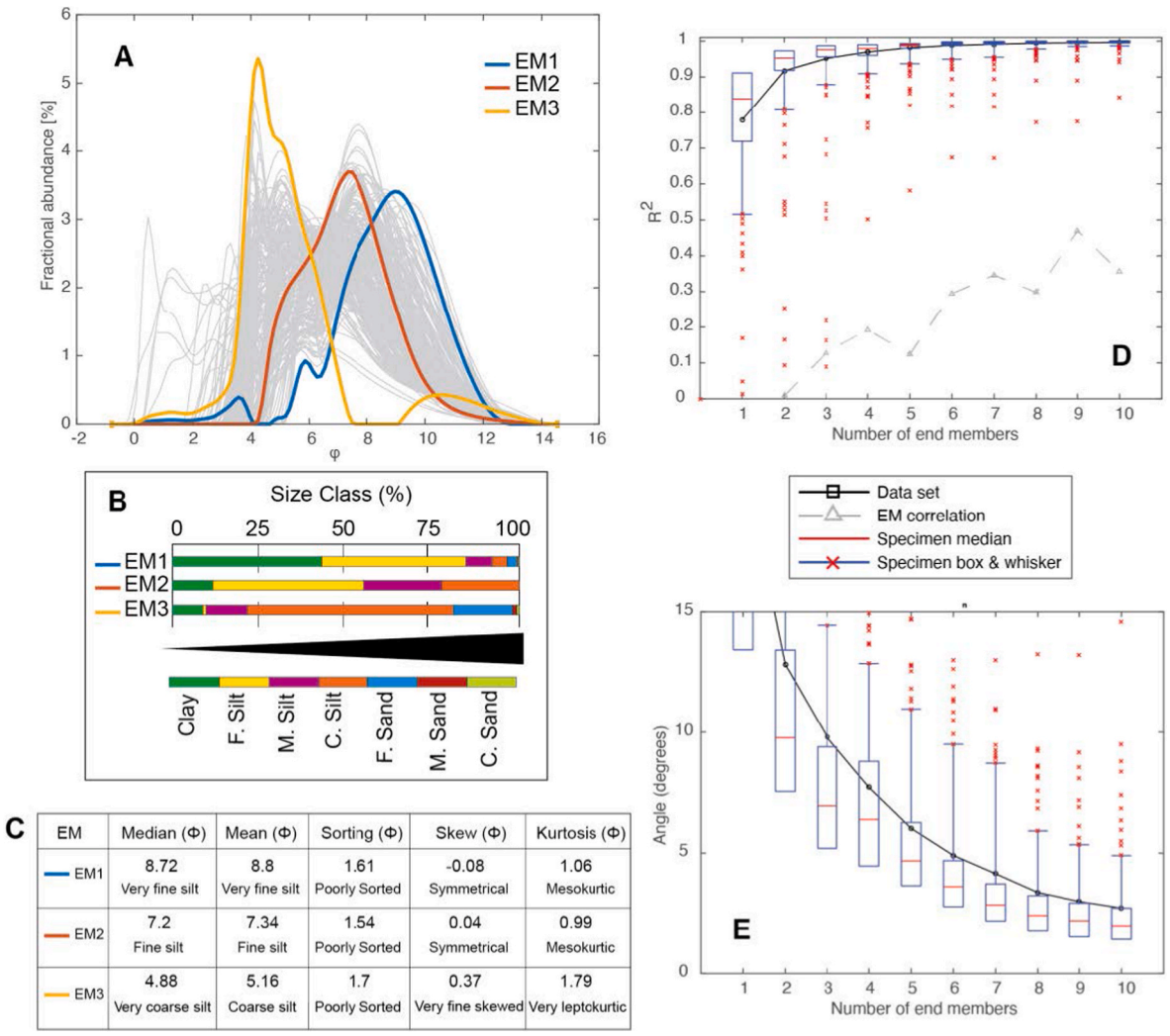
The sedimentary sequence at Nyayanga has been divided into three units (NY-1 to NY-3), which vary laterally over a ~200 m transect. Fig. 3 displays the individual geotrench (GT) sedimentary logs with the lateral extent of sedimentary units NY-1 to NY-3. NY-4 is found disconformably above NY-3 in most locations across Nyayanga. However, due to its erosive contact, it has not been analysed in detail for this study. Of the nine trenches, we provide detailed logs, particle size data, and vegetation reconstructions for eight (Fig. 4). Logs are presented to show sediment thickness, sediment type, particle size distribution, EM abundance, and phytolith-inferred vegetation types. Phytolith preservation was variable, but in each sample, we managed to reach the minimum 200 counts. More detailed phytolith morphotypes are available in the supplementary figures (see Supplementary Material). Following this, we present a composite summary sedimentary log of the Nyayanga units (Fig. 5), which demonstrates the overall sedimentary sequence and places the artefact and faunal finds from Plummer et al. (2023) and Finestone et al. (2025) into this sedimentological framework (see excavation labels on Fig. 5). Excavation 3, from which most artifacts and faunal remains were discovered, lies within NY-1 and based on the below descriptions is primarily from within subunits NY-1C or NY-1D.

4.1. Defining end-members for quantifying particle size distributions

At Nyayanga, a three EM model was chosen to best represent the dataset without overfitting (Fig. 2). A high coefficient of determination ($r^2 = 0.952$) and a 95th percentile was obtained with this model, while maintaining a low linear correlation between the EMs ($r^2 = 0.138$). A low angular deviation was obtained ($\theta = 9.759$), indicating the angular difference in degrees between the reconstructed and observed data. A sample with a high R^2 and/or a low angular deviation suggests that the EM model has accurately represented the sample. EM densities were exported from the AnalySize measurement software (Paterson and Heslop, 2015) and imported into GRADISTAT program (Blott and Pye, 2001) to compute descriptive statistics and size classes to maintain consistency with the original particle size distributions. Here we present the characteristics and interpretation of each end-member, the proportion of which is then described for each sedimentary unit.

EM1 is a symmetrical, poorly sorted silty clay with a mean and median grain size of 8.8 Φ, and is mesokurtic, with a coarse tail incorporating minimal fine sand (Fig. 2). EM1 often occurs in conjunction with matrix-supported granules, pebbles, and cobbles, some of which are carbonaceous. These carbonates are individual clasts and lack evidence of laminae or coalescence, indicating that they are not *in situ* and are reworked (Machette, 1985), and could have formed in flow hiatuses. Although much of EM1 is composed of fine sediment, EM1's association with clasts and coarser particles suggests that it is not a low-energy environment (Pierson, 2005). The poor sorting of EM1 and the absence of sedimentary structures indicate that these sediments were deposited rapidly under a variable flow regime, or were infrequently reworked (McLaren and Bowles, 1985; Blott et al., 2004). These characteristics indicate viscous, sediment-rich hyperconcentrated flows, which occurred quickly and infrequently, and were unconfined. Erosive features are often absent in such instances, as the viscous nature and low shear stress bases of these flows frequently bury rather than erode the underlying sediment. EM1 also appears to be multimodal, a common feature of hyperconcentrated flows (Pierson, 2005).

EM2 is slightly coarser than EM1 and is a symmetrical, poorly sorted silt (Fig. 2). It has a unimodal distribution and a mean grain size of 7.34 Φ. The highest percentages of EM2 are most frequently associated with sediments lacking coarse particles and sedimentary structures. In some areas, high percentages of EM2 are related to the presence of coalescing carbonate nodules and *in situ* carbonate nodules. This suggests that EM2



C

EM	Median (Φ)	Mean (Φ)	Sorting (Φ)	Skew (Φ)	Kurtosis (Φ)
EM1	8.72 Very fine silt	8.8 Very fine silt	1.61 Poorly Sorted	-0.08 Symmetrical	1.06 Mesokurtic
EM2	7.2 Fine silt	7.34 Fine silt	1.54 Poorly Sorted	0.04 Symmetrical	0.99 Mesokurtic
EM3	4.88 Very coarse silt	5.16 Coarse silt	1.7 Poorly Sorted	0.37 Very fine skewed	1.79 Very leptokurtic

Fig. 2. Plots for particle size distributions for End Members at Nyayanga. (A) The three EM models overlaid on particle size distributions from Nyayanga geotrench samples: (B) Size fractions of each EM, (C) Textural parameters of each EM, (D) Linear correlations for each EM scenario, and (E) Angular deviations for each EM scenario.

relates to a low-energy, infrequently reworked, depositional environment, stable enough for soil development to take place (Folk and Ward, 1957; Machette, 1985; Liu et al., 2014). EM2, therefore, likely represents periods of flow hiatuses or landscape stability at Nyayanga. This aligns with the interpretation of EM1, as hyperconcentrated flows are often separated by periods of landscape stability and pedogenic development. During these stable periods, sedimentation occurred as fluvial runoff and aeolian deposition (Vandenberghe, 2013; de Haas et al., 2014).

EM3 is a poorly sorted, very fine sandy silt with a mean grain size of 5.16 Φ (Fig. 2). Although classed as a unimodal distribution in GRADISTAT, it has a small fine peak incorporating clay alongside its coarser primary peak. For this reason, the median (4.88 Φ) may be more appropriate for classifying the average grain size, which can be identified as very coarse silt. The kurtosis of EM3 is higher than that of previous EMs; it is classified as very leptokurtic, suggesting that its central peak of coarse silts is better sorted than the distribution's tails. The higher percentages of coarse silt and sand characterising EM3 indicate that it represents mechanisms associated with higher transport and depositional energy than EM2. EM3 is often associated with matrix-supported gravel, which incorporates granules and pebbles. These clasts are frequently carbonaceous but show little evidence of coalescing or the development of laminae, again suggesting that they are reworked (Machette, 1985). Sedimentary structures, including erosive contacts and faint laminations, can also be observed, pointing towards fluvial/alluvial activity; however, no channel features are evident (Miall, 2013). Like previous EMs, EM3 is poorly sorted, suggesting that it may have been rapidly deposited or deposited under a variable flow regime (McLaren and Bowles, 1985). Given the presence of laminations, deposition under a variable flow regime is more likely, as rapid deposition would result in massive structureless deposits (Pierson, 2005; Miall, 2013; North and Davidson, 2012). This suggests that EM3 represents unconfined fluvial flows that periodically had sufficient energy to entrain coarser sediment. Matrix-supported deposits are thought to be the result of flow deceleration as flows expanded and the concentration of suspended sediment increased, causing the flow to become hyperconcentrated and more debris flow-like (North and Davidson, 2012).

4.2. *Sedimentary units and phytoliths*

4.2.1. *NY-1*

The lowermost sedimentary unit at Nyayanga, NY-1, was deposited between 3.05 and 2.60 million years ago (Plummer et al., 2023). The unit's lithology varies laterally, though broadly composed of grey clay to silt-rich deposits interbedded with orange sands, the latter associated with granules to cobbles. As shown by Plummer et al. (2023), NY-1 exhibits an overall fining upward sequence, however due to the highly variable lithology of this unit, subunits have been defined (NY1A-E).

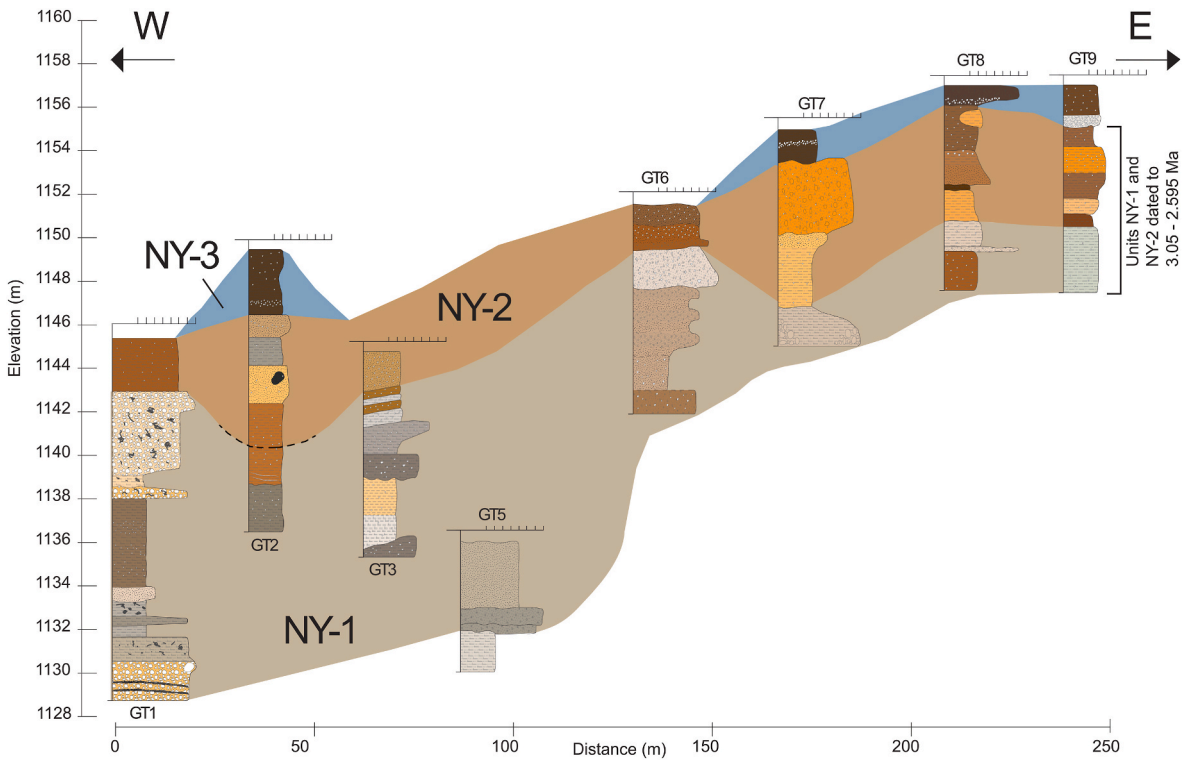


Fig. 3. Sedimentary units identified site-wide at Nyayanga across geotrenches. The vertical placement of trenches represents their elevation at the site. Horizontal placement of trenches represents their position from west to east of the site. Precise locations of each Geotrench are shown in Fig. 1B.

NY-1A: NY-1A is characterised by clasts up to cobbles in size suspended in a fine clayey silt matrix. There is often a clast-supported cobble layer at the base of this unit, where it is erosively unconformable with the underlying Homa Formation. EM2 dominates, although EM1 is present up to 45%. Massive, poorly sorted matrix-supported clasts and high abundances of EM1 and EM2 indicate that the sediments are episodic hyperconcentrated flow deposits, separated by periods of landscape stability. During these quiescent periods, deposition took place via secondary processes, including fluvial runoff and aeolian deposition (Pope and Wilkinson, 2005; Harvey et al., 2005; Vandenberghe, 2013).

The phytolith assemblage is dominated by grass and generalist phytoliths, while trees, shrubs and sedge phytoliths are present but in low percentages. This suggests that the landscape was dominated by grasses with scattered trees & shrubs (~15%), resembling an open-canopied vegetation structure.

NY-1B: These sediments include interbedded massive muddy matrix-supported pebbles and massive mud. EM1 and EM2 are dominant, although EM3 is present. The shift from NY-1A to NY-1B suggests that the depositional environment became highly variable. Massive muddy matrix-supported pebbles are characteristic of hyperconcentrated and debris-rich flows (Pierson, 2005). Clast abundance is laterally variable, reflecting spatial variability in flow activity and strength. The lower abundance of EM2 indicates that the development of stable land surfaces did not occur as frequently as in NY-1A. With the absence of channel features and the increase of EM3, unconfined fluvial activity became more frequent and capable of eroding and entraining sand-sized sediment, and as indicated by the rise in EM3, fluvial runoff and aeolian deposition occurred at times (Vandenberghe, 2013). The absence of hyperconcentrated flows in the lower massive muds may reflect increased precipitation, as fine sediment may have been reworked more often (de Haas et al., 2014). In some locations, greater sediment accumulation and lighter-coloured carbonaceous sediment indicate that these sediments were deposited on a relatively stable land surface, with soil development occurring.

Grass- and generalist phytoliths are most abundant in this subfacies. In GT1 and GT3, trees, shrubs, and sedge-derived phytoliths reach their highest site-wide abundance (~15%). However, they are almost absent in GT5 and GT6. The phytolith variability through this subunit suggests a transient depositional environment with periods of landscape stability.

NY-1C: These sediments are characterised by poorly sorted massive silty sands that have an erosive contact with the underlying massive muds. EM2 and EM3 are most abundant throughout. GT1 and GT5 are dominated by EM3, accounting for ~50% of the EM composition, while in GT3 and GT6, EM2 is most abundant. EM1 is poorly represented throughout this subunit, with a representation of ~25% or lower at all sites. This subunit indicates a shift to a more frequently wet environment, with the sediment's erosive contacts suggesting the presence of more water-laden flows. The presence of coarse sand is product of erosional events, which may explain why they are not observed in the underlying hyperconcentrated flow sediments, as these flows are more likely to bury sediments than erode them. The coarse sands observed in NY-1C are thought to be sourced from the weakly cemented sandstones underlying NY-1. The absence of channel features and the higher abundances of EM3 suggest that the flows were unconfined. EM2 is also abundant throughout these sediments, though carbonate nodules are absent, suggesting that periods of landscape stability were short-lived. As a result, unconfined fluvial activity might have been intermittent and possessed a variable flow regime (McLaren and Bowles, 1985; Blott et al., 2004).

These sediments are characterised by grass and generalist-derived morphotypes, indicating an abundance of grasses with sparse woody species. Such vegetation is commonly associated with unconfined flows. The presence of sedges suggests that the landscape experienced occasional seasonal or local flooding.

NY-1D: Sediments in this subunit are broadly characterised by massive grey-brown clayey silts with carbonate nodules and occasional granules. In GT3, sediments are slightly coarser and characterised by massive orange-brown sandy silts with carbonate nodules. In GT1, GT2, and GT8, NY-1D consists of a massive, grey to red-brown silt with

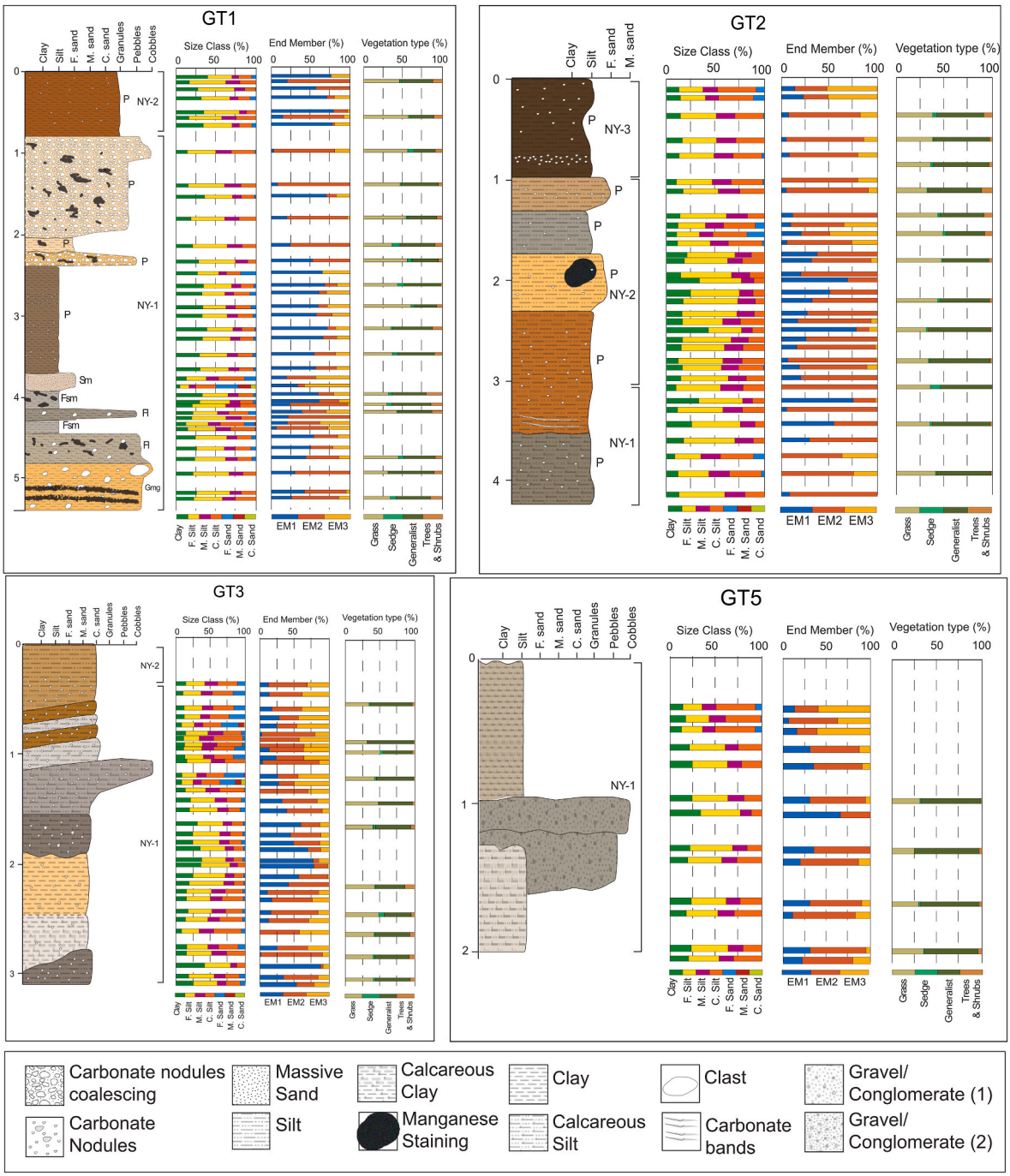


Fig. 4. Sediment logs of geotrenches 1, 2, 6, 7, 8, and 9 at Nyayanga. Sediment log depth is presented in metres. Facies codes outlined by Miall (2013) are included in sediment logs. Particle size distributions, EM abundances, and vegetation types are also included at corresponding sample depths.

carbonate nodules. The dominance of EM2 in NY-1D suggests the environment was characterised by more frequent periods of landscape stability than the underlying sediments, with carbonate nodules suggesting that these periods were sufficiently sustained for soil development. The reduction in EM3 indicates that high-energy fluvial activity was less frequent, and deposition occurred through low-energy fluvial runoff (de Haas et al., 2014). This is supported by the absence of coarser sands and an overall decrease in sand content. Whilst sediment exhaustion may also explain the general reduction in sand content observed, the development of stable land surfaces, evidenced by the presence of EM2 and carbonate development, suggests that it was due to a decrease in flow velocity.

High percentages of grass and generalist phytoliths characterise the phytolith assemblage in this subunit. Sedge phytoliths are also present but in low percentages (<10%). Woody phytoliths are absent except for the GT1 subunit, where they are present in low percentages (<10%). This indicates the continuation of an open landscape, characterised by abundant grasses and forbs with less frequent trees, shrubs, and sedges.

NY-1E: NY-1E is sedimentologically variable but broadly characterised by carbonaceous clayey silts containing carbonate nodules. It is massive, varying from light orange to grey, and contains coalescing carbonate nodules of varying sizes, up to pebble-sized. EM2 is dominant throughout most exposures. EM3 is also present in all exposures, typically with an abundance of 30% or less. EM1 is almost absent from all

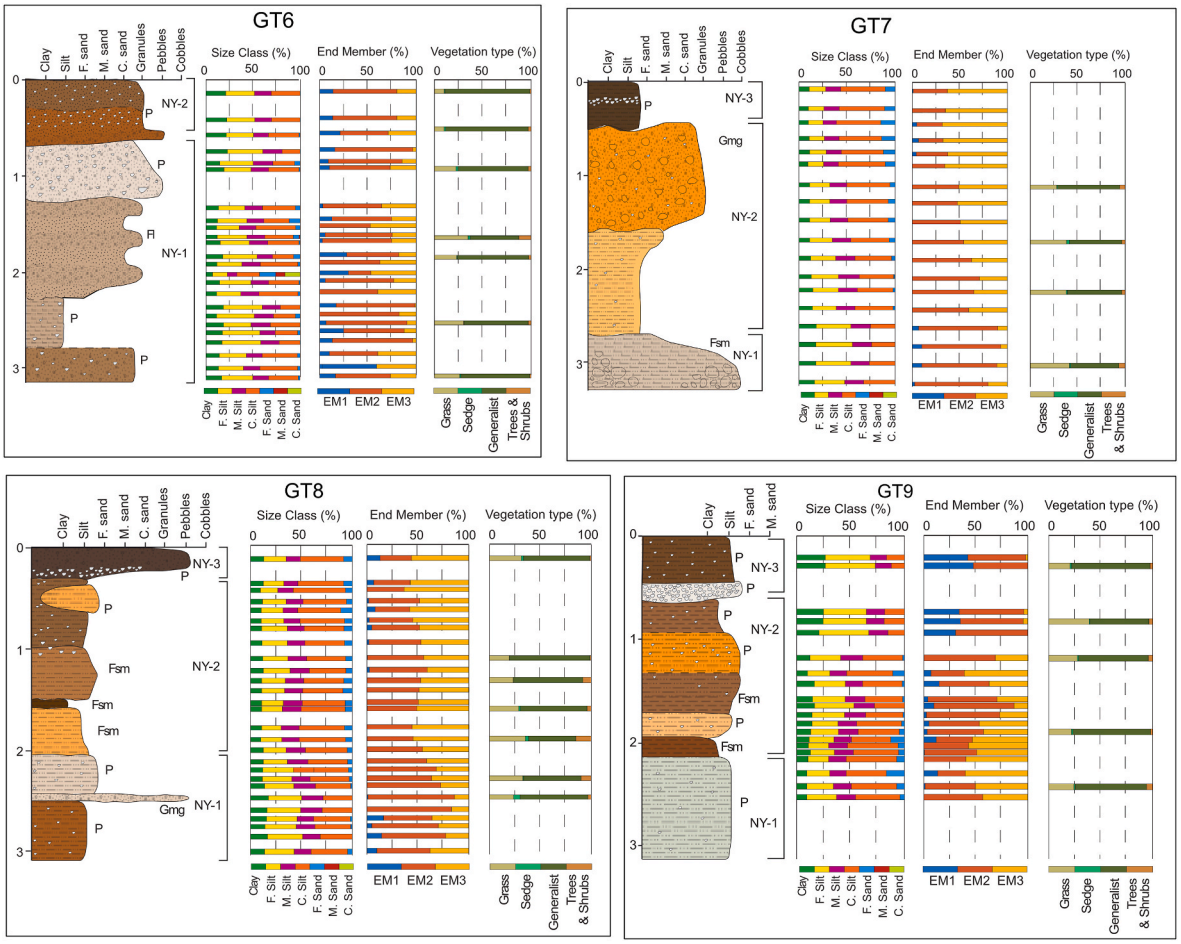


Fig. 4. (*continued*).

exposures except for GT1. The carbonaceous sediment and the frequent coalescent carbonate nodules indicate that periods of landscape stability were sufficiently long for significant pedogenic development to occur and reach relatively mature stages (Ditchfield et al., 1999). The sedimentological dominance of EM2 supports this. The presence of EM3 and the absence of channel features suggest that unconfined fluvial activity still occurred at times, potentially through fluvial runoff.

The phytolith assemblage in this subunit is characterised by abundant grass and generalist phytoliths. Woody- and sedge-derived phytoliths are infrequent, with a percentage lower than 10%. This suggests the persistence of an open landscape characterised by abundant grasses and forbs.

4.2.2. NY-2

NY-2 is well-exposed throughout Nyayanga, with the exception of GT5. The sediments of NY-2 were deposited after those of NY-1, but still between 3.05 and 2.595 Ma (Plummer et al., 2023). Most commonly, NY-2 is a massive, red-brown, strongly pedogenically altered clayey silt with sandy intercalations of coarse sand to granules, much of which is stained with manganese. NY-2 is divided into five subunits (A to E), which reflect lateral variation within the unit.

NY-2A: This subunit is characterised by massive clayey silts with pedogenic carbonates. Sediments are red-brown and occasionally incorporate granule-grade clasts in some areas (GT6). EM characteristics throughout this subunit exhibit high lateral variability. The absence of sedimentary structures and larger clasts, along with the reduced percentage of sand, indicates that the lowermost sediments of NY-2A were characteristic of a low-energy environment. The presence of EM2 throughout this subunit supports this and suggests that stable land surfaces were common. Carbonate nodules indicate some soil development during this period, although the lack of coalescence or development of laminae suggests these were not mature soils. The absence of channel features, combined with the frequency of EM3, indicates that low-energy, intermittent, and unconfined fluvial activity continued. As with the uppermost sediments of NY-1, a reduction in the frequency of EM3 from the southeast of the site at GT9 to the northwest at GT1 occurs, suggesting the most active area of these flows remained in the southeast.

Phytoliths throughout this subunit are dominated by generalist phytoliths in all trenches, except for GT1, where grass-indicating phytoliths are dominant. Throughout, woody and sedge indicating phytoliths are rarely present. This suggests a landscape characterised by an abundance of bushes, grasses, and forbs. The absence of both trees and sedges suggests a possible phase of increased aridity (Tipple and Pagani, 2007; Ségalen et al., 2007; Cerling et al., 2013; Maslin et al., 2014).

NY-2B: This subunit is characterised by massive, orange-grey, clayey silts with carbonate nodules and light cementation. EM1 is only present in GT2, where it fluctuates between 25% and 75%. EM2 is more abundant throughout most of the exposure, while EM3 is almost entirely absent. In all other exposures, EM2 and EM3 account for the subunit's entire composition. The dominance of poorly sorted clayey silts containing carbonate nodules suggests a low-energy environment that allowed soil formation. The degree of cementation associated with these sediments suggests that the soils were more mature than those in the underlying sediments and better developed than in the NY-2A subunit. Abundances of EM2 agree with this interpretation, with common periods of stable land surface development. An increase in sand content and the presence of EM3 suggest a wetter environment, as unconfined

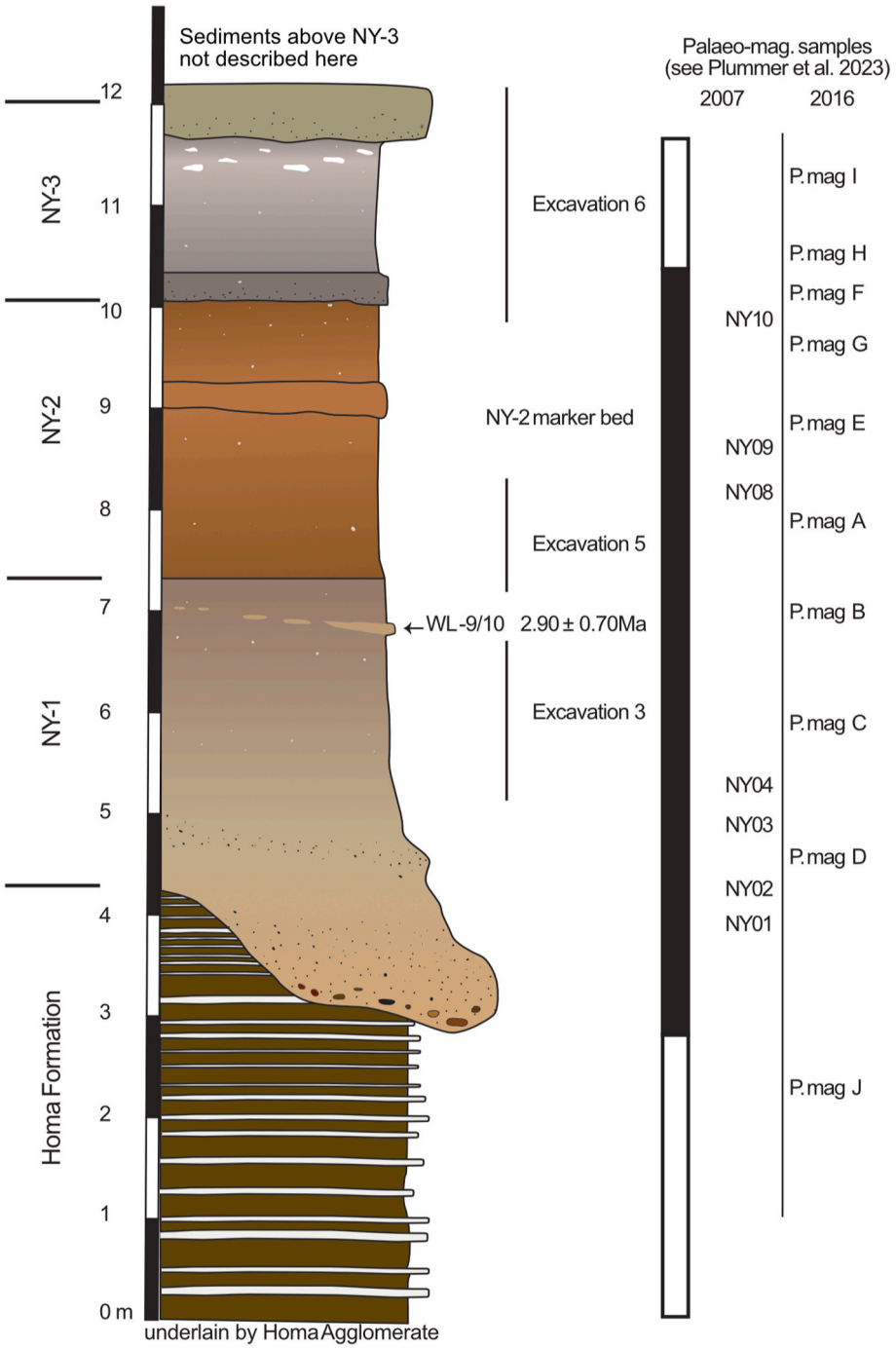


Fig. 5. Composite sedimentary log from Nyayanga, showing Homa Formation and NY-1 to NY-3. Location of excavations reported in Plummer et al. (2023) is shown, alongside key chronological control (Plummer et al., 2023).

fluvial activity appears more common, with a higher entrainment capacity. EM3 follows the same trend of decreasing abundance from southeast to northwest, suggesting that this is where flow deceleration of unconfined flows may have occurred.

Grass and generalist phytoliths are most abundant in these sediments. Woody and sedge phytoliths are present but in low amounts (less than 15%). The increase in woody vegetation and sedges compared to NY-2A indicates a slightly wetter environment, but not to the point of shifting the vegetation structure; grasses with scattered trees & shrubs persisted.

NY-2C: Sediments in this subunit vary laterally. In GT7, NY-2C sediments are characterised by orange sandy silts supporting pebbles and carbonate nodules. EM3 is most dominant and increases in abundance upward through the subunit. EM2 is present throughout and displays the opposite trend, whilst EM1 is largely absent. At GT8, there is a reduction in sand content, and sediments are composed of light brown silts. EM2 and EM3 are equally abundant throughout, while EM1 is absent. In GT9, sand content is further reduced, and sediments are characterised by brown clayey silts, which lighten in colour to orange clayey silts incorporating carbonate nodules. EM1 is absent, with EM2 and EM3 being the dominant ones. EM2 is most abundant at GT9, although EM3 is dominant in the upper part of this subunit. Within NY-2C, the increasing abundance of EM3, the increase in sand content, the presence of pebbles, and the lack of channel features indicate that

unconfined fluvial activity was more frequent and of higher velocity. The relatively steady abundance of EM2 highlights that these flows remained intermittent and were characterised by periods of stable land development in flow hiatuses. The presence of carbonate nodules in these sediments is indicative of soil development. However, the lack of laminae or coalescence suggests these were immature or potentially reworked by the intermittent unconfined fluvial activity.

Generalist phytoliths dominate this subunit throughout. Grass phytoliths are present, accounting for ~25%. Woody phytoliths are present in low proportions (<10%), whilst sedge phytoliths are absent. This indicates open grasslands mixed with forbs.

NY-2D: NY-2D is poorly exposed throughout Nyayanga, only visible in GT2 (1.7 m – 1.3 m below ground level) and GT8 (1 m – 0.3 m below ground level). The lower part of this unit is composed of grey-orange granular silts with carbonate nodules, and the upper part is characterised by orange-brown silts and increased amounts of carbonate nodules. EM2 and EM3 are present in relatively equal abundances for the lower part of this unit, whilst EM2 becomes dominant (>75%) in the upper parts. EM1 is present in very low percentages throughout the unit, below 15%. The sediments suggest relative environmental consistency through their extent. Relatively equal abundances of EM2 and EM3 indicate intermittent unconfined flow events, with flow hiatuses marked by periods of stable land development. Although the presence of carbonate nodules throughout these sediments indicates soil development, the lack of laminae and coalescence again suggests that soil development here is moderately immature or that nodules have been reworked.

Grass and generalist phytoliths are most prominent throughout this unit. Grass phytoliths have a slightly higher proportion in the lower parts, whilst generalist phytoliths are more abundant in the upper parts. However, overall, there is no significant variation in vegetation structure, likely due to the undeveloped soil structure, which cannot support wooded vegetation.

NY-2E: NY-2E is only visible in GT2 (1.3 m – 1 m below ground level) and through some of the excavations (not described here), though GT2 is the only location in which it is seen in stratigraphic position. It is found directly over NY-2E and is a well sorted light beige silt containing carbonate nodules, dominated by EM2 (>75%). EM1 is present in low percentages (<15%) throughout. Initial analysis indicates this is a volcanic tuff, with the glass component diagenetically altered to clay (A. Deino, personal communication, 2026). Grass and generalist phytoliths are most prominent throughout this unit.

4.2.3. NY-3

NY-3 is exposed through several locations, characterised by massive brown silts with pedogenic carbonates, sometimes coalescing to form cemented horizons. EM2 and EM3 compose much of this unit. EM3 dominates GT7 and GT8, while EM2 dominates GT9 and much of GT2. EM1 is present in all exposures at low abundances, except in GT9, where it is particularly abundant (>40%). The environment of NY-3 was characterised by lengthy periods of stable land formation, which allowed for soil development, as evidenced by the abundance of pedogenic carbonates. These carbonates display evidence of a higher degree of maturity, including coalescence and the formation of laminae and thick horizons. The presence of sand-sized sediment, the absence of channel features, and the high abundance of EM3 suggest that unconfined fluvial activity continued in this unit.

Similarly to NY-2, generalist phytoliths dominate this unit, whilst grass phytoliths exhibit moderate abundance (~30%). Wood and sedge indicate that phytoliths are present in low percentages (less than 10%). Overall, NY-3 vegetation cover is characterised by open grasslands with scattered trees and shrubs and a low presence of sedges.

4.3. Isotopic results and interpretations

Pedogenic carbonates and woody cover: Woody cover estimation indicates that grassy woodland/bushland/shrubland (~40-60% woody cover) was the dominant vegetation type while NY-1 pedogenic carbonates were forming approximately 40 m from the palaeochannel (Fig. 6). Pedogenic carbonates from NY-2 and NY-4 indicate a reduction in woody cover associated with grasslands and wooded grasslands (woody cover <40%) in comparison to those collected from NY-1. The woody cover estimates presented here (based on the eastern Africa-specific woody cover model), are 9-13% higher than estimates reported in Plummer et al. (2023) that were based on the global model (Cerling et al., 2011). However, given the wide range in both models, the estimates are in relatively good agreement. There is no significant difference in the oxygen isotope composition of pedogenic carbonates from NY-1 ($\delta^{18}O = -2.7 \pm 0.8‰$, mean $\pm 1\sigma$), NY-2 ($\delta^{18}O = -2.9 \pm 1.0‰$), and NY-3 (−2.3‰), indicating no significant change in the controls of pedogenic carbonate $\delta^{18}O$ such as soil water evaporation and moisture source; thus, vegetation change up the Nyayanga sequence may be related to other factors. It should be noted that this is a small sample size, and there may be additional lateral variation and variation through the stratigraphic sequence which is not identified by these samples.

Palaeoseasonality: Stable isotope results from serial sampled *Eurygnathohippus* teeth from NY-1, including an upper molar (NY15-40) and a lower molar (NY15-29), are presented in Fig. 7 and Table 1. From tspecimen NY15-40, a total of 17 subsamples were collected with increasing distance from the occlusal surface (0.1 to 7.2 cm). The average $\delta^{13}C$ is 0.7‰ across all subsamples, and $\delta^{13}C$ varies throughout the tooth from −0.3‰ to 1.4‰ (intratooth $\delta^{13}C$ range = 1.7‰), indicating a consistent C_4-grazing diet throughout the enamel formation period of this tooth. The $\delta^{18}O$ average is 0.9‰ and varies from −1.3‰ to 2.1‰ (intratooth $\delta^{18}O$ range, not corrected for the damping factor = 3.4‰). From the *Eurygnathohippus* specimen NY15-29, 14 subsamples were collected with increasing distance from the occlusal surface (0.1 to 5.9 cm). The average $\delta^{13}C$ is −0.9‰ across all subsamples, varying from −1.7‰ to −0.3‰ (intratooth $\delta^{13}C$ range = 1.4‰), indicating a consistent C_4-grazing diet throughout the enamel formation period of this tooth. The $\delta^{18}O$ average is 0.9‰ and varies from −1.3‰ to 2.1‰ (intratooth $\delta^{18}O$ range. not corrected for the damping factor = 3.4‰).

When considering these results, as well as previously published results from intratooth isotopic sampling of an *Eurygnathohippus* molar (Plummer et al., 2023), the average intratooth oxygen isotope range of NY-1 fossil equid teeth (n = 3) at Nyayanga is 2.2‰. After correction

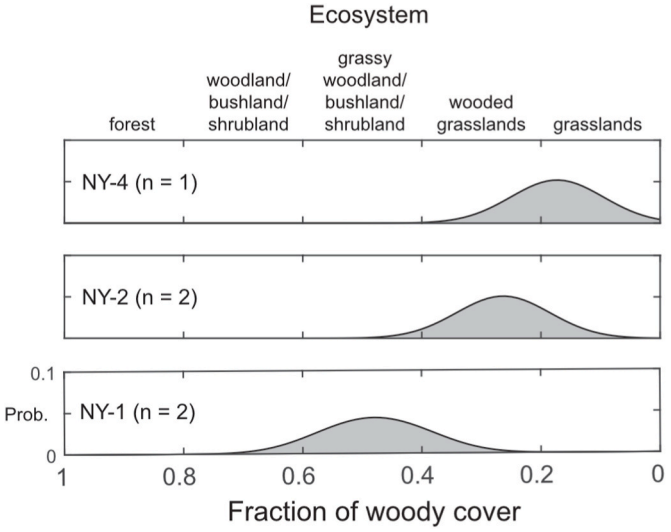


Fig. 6. Normalised probability density functions of estimated woody cover fraction, based on previously published carbon isotope composition of pedogenic carbonates from NY-1, NY-2, and NY-4 (Plummer et al., 2023), following the approach developed by (Cerling et al., 2011) and revised for eastern African ecosystems by (Negash et al., 2024).

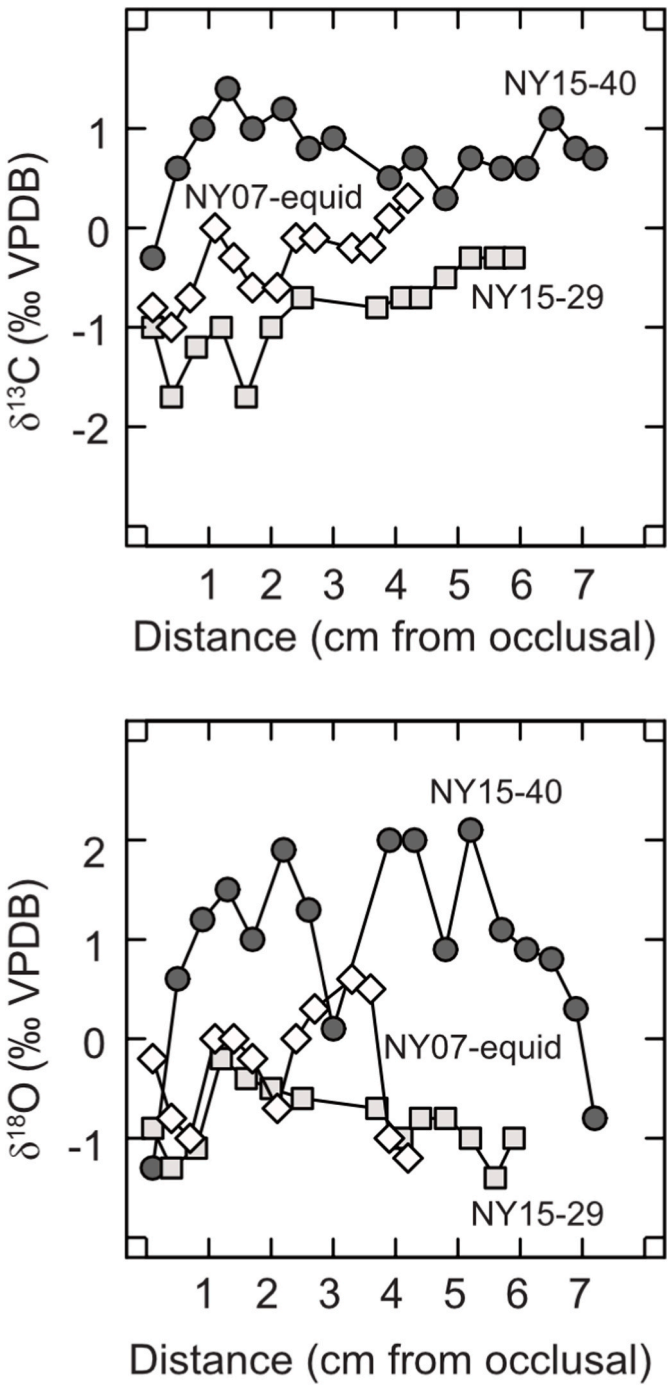


Fig. 7. Intratooth carbon and oxygen isotope profiles from NY-1 fossil equids. Two profiles (NY15-40 and NY15-29) are from this study, and the NY07-equid profile is previously published (Plummer et al., 2023).

using the damping factor, the predicted intratooth $\delta^{18}O$ range is 4.6 ± 0.7‰, which corresponds to an intra-annual precipitation $\delta^{18}O$ range of approximately 4‰ (Fig. 8) and is within the range of variation at other Early Pleistocene sites on the Homa Peninsula (Kanjera South) and from northern Tanzania (e.g. Olduvai Bed I, Blumenthal et al., 2019). Palaeoaridity estimates for NY-1, based on oxygen isotope comparisons of evaporation-sensitive and insensitive mammalian herbivore taxa, indicate a moderately negative (i.e. mesic) annual water deficit within the range of other Pliocene-Pleistocene fossil collections (Plummer et al., 2023). Thus, NY-1 climatic conditions appear to have included seasonal changes in moisture source and/or rainfall amount with annually relatively cool and/or wet conditions.

Table 1
Summary of intratooth isotopic sampling of fossil equid molars. Isotopic measurements are presented in per mil (‰) notation relative to Vienna Pee Dee Belemnite (V-PDB).

Specimen ID	Taxon	Dist. from occl. surf (cm)	$\delta^{13}C$ (VPDB)	$\delta^{18}O$ (VPDB)
NY15-29	*Eurygnathohippus*	0.7	−1	−0.9
NY15-29	*Eurygnathohippus*	0.06	−1.7	−1.3
NY15-29	*Eurygnathohippus*	0.42	−1.2	−1.1
NY15-29	*Eurygnathohippus*	0.78	−1	−0.2
NY15-29	*Eurygnathohippus*	1.20	−1.7	−0.4
NY15-29	*Eurygnathohippus*	1.64	−1	−0.5
NY15-29	*Eurygnathohippus*	2.02	−0.7	−0.6
NY15-29	*Eurygnathohippus*	2.48	−0.8	−0.7
NY15-29	*Eurygnathohippus*	3.71	−0.7	−1
NY15-29	*Eurygnathohippus*	4.10	−0.7	−0.8
NY15-29	*Eurygnathohippus*	4.43	−0.5	−0.8
NY15-29	*Eurygnathohippus*	4.82	−0.3	−1
NY15-29	*Eurygnathohippus*	5.22	−0.3	−1.4
NY15-29	*Eurygnathohippus*	5.63	−0.3	−1
NY15-29	*Eurygnathohippus*	5.90	−1	−0.9
NY15-40	*Eurygnathohippus*	0.14	−0.3	−1.3
NY15-40	*Eurygnathohippus*	0.53	0.6	0.6
NY15-40	*Eurygnathohippus*	0.90	1	1.2
NY15-40	*Eurygnathohippus*	1.33	1.4	1.5
NY15-40	*Eurygnathohippus*	1.73	1	1
NY15-40	*Eurygnathohippus*	2.18	1.2	1.9
NY15-40	*Eurygnathohippus*	2.60	0.8	1.3
NY15-40	*Eurygnathohippus*	3.05	0.9	0.1
NY15-40	*Eurygnathohippus*	3.92	0.5	2
NY15-40	*Eurygnathohippus*	4.34	0.7	2
NY15-40	*Eurygnathohippus*	4.78	0.3	0.9
NY15-40	*Eurygnathohippus*	5.19	0.7	2.1
NY15-40	*Eurygnathohippus*	5.68	0.6	1.1
NY15-40	*Eurygnathohippus*	6.13	0.6	0.9
NY15-40	*Eurygnathohippus*	6.55	1.1	0.8
NY15-40	*Eurygnathohippus*	6.94	0.8	0.3
NY15-40	*Eurygnathohippus*	7.22	0.7	−0.8

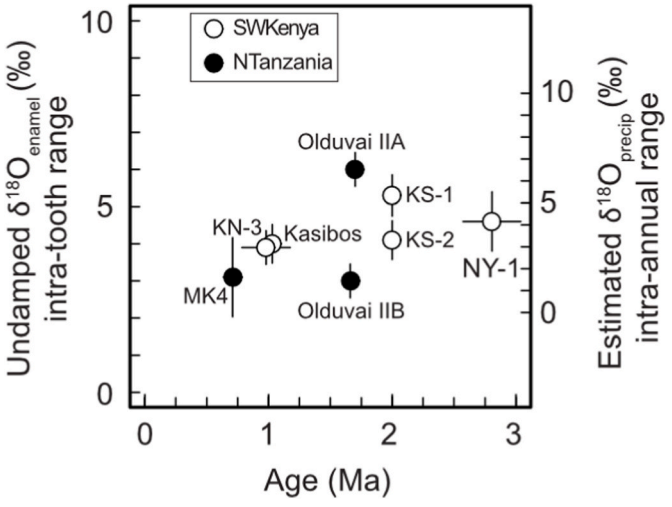


Fig. 8. Intratooth ranges in enamel oxygen isotope measurements and estimated intra-annual oxygen isotope ranges of ancient precipitation for Nyayanga equids. For comparison, we also show previously published intratooth ranges from fossil equid teeth from Kanjera North (KN-3), Kanjera South (KS-1 and KS-2), Kanam East (Kasibos Formation), Olduvai Gorge Bed IIA (between Tuff IIA and Tuff IIB) and IIB (between Tuff IIB and Tuff IIC), and the Manyara Beds (MK4) in the Makuyuni area in northern Tanzania. Uncertainty represents the propagation of standard errors associated with the $\delta^{18}O$ range for each site and the regression model used to estimate undamped from measured intra-tooth $\delta^{18}O$ ranges.

5. Discussion

5.1. Depositional environment reconstruction

Our multi-proxy reconstruction suggests that the depositional environment at Nyayanga was characterised by a combination of hyperconcentrated flows, intermittent unconfined fluvial activity with variable energy regimes, and flow hiatuses in which aeolian deposition and stable land development occurred (Table 2). This primarily happened across an open landscape on the distal slopes of Homa Mountain and is indicative of an alluvial fan/plain environmental setting (Blair and McPherson, 1994a, 1994b; Harvey et al., 2005; North and Davidson, 2012; Mather et al., 2017; Mather and Hartley, 2005). The evidence of first hominin activity at Nyayanga is found in Excavation 3, defined here as during the deposition of subunits NY-1C to NY-1D (Fig. 5, Table 2, Plummer et al., 2023), a period characterised by a wetter environment followed by progressive increased environmental stability. Hominin activity has been identified in this type of environment elsewhere during the Plio-Pleistocene of eastern Africa (Brown, 1984; Feibel and Brown, 1991; Hay and Kyser, 2001; Ashley et al., 2009; Uribelarrea et al., 2017; Patterson et al., 2017).

Table 2
Summary of palaeoenvironmental characteristics interpreted for each sedimentary unit and subunit identified at Nyayanga.

Unit	Subunit	Palaeoenvironment characteristics
NY-1	NY-1A	Episodic hyperconcentrated flows capable of entraining cobble-grade sediment. Flow hiatuses are characterised by land surface development, fluvial runoff, and aeolian deposition. Open bushy grassland with infrequent woodland and sedges.
	NY-1B	Deposition fluctuates between episodic hyperconcentrated flows and intermittent unconfined fluvial flows capable of eroding underlying sediment. Flow hiatuses are characterised by landscape stability and secondary processes. Open bushy grasslands with infrequent woodland and sedges.
	NY-1C	Shift to a wetter environment. Intermittent unconfined fluvial flows with a variable flow regime. Flow hiatuses were not lengthy enough for significant pedogenesis. A similar palaeovegetation structure remained.
	NY-1D	Increased environmental stability characterised by pedogenic development and secondary processes, including fluvial runoff and aeolian deposition. Intermittent unconfined flows. Bushy grasslands with infrequent woodland and sedges persisted.
	NY-1E	Increasing environmental stability with significant soil maturity. Infrequent unconfined low-energy fluvial flows. Secondary processes characterise flow hiatuses. Bushy grassland/grassy bushlands characterise palaeovegetation
NY-2	NY-2A	Low energy environment with frequent periods of landscape stability. Intermittent unconfined fluvial activity occurred, potentially attributable to secondary fluvial runoff. Landscape characterised by grassy bushlands
	NY-2B	An increasingly stable environment with soil development reaching advanced stages of maturity. Intermittent unconfined fluvial activity occurred throughout, characterised by higher transport energy, suggesting a wetter environment. An increase in woodland and sedges, though the landscape remained dominated by grassy bushlands.
	NY-2C	Unconfined fluvial activity became more common and increased in flow velocity but remained intermittent. Flow hiatuses are characterised by stable land development and early stages of pedogenesis. Grassy bushlands characterised the landscape.
	NY-2D	Intermittent unconfined fluvial activity with stable land surface development in flow hiatuses. Early stages of pedogenesis. Palaeovegetation characterised by bushy grasslands/grassy bushlands with infrequent woodland and sedges
NY-3	-	A stable environment in which mature soils have developed with the late stages of pedogenesis. Unconfined fluvial activity occurred intermittently. Grassy bushlands with infrequent woodland and sedges characterise the palaeovegetation.

Alluvial plains form between highlands and depositional lows, where highlands function as sediment sources while depositional lows provide ample accommodation space for sediment accumulation. The rapid elevation changes from Homa Mountain towards the expansive depositional low in the west make Nyayanga a likely area for this formation (Le Bas, 1977; Blair and McPherson, 1994b; Harvey et al., 2005), with the thicker exposure of sediments in the northwest of the site representing a depositional sink with greater accommodation space for sediments to accumulate.

Alluvial environments are also frequently characterised by episodic mass flow and/or unconfined fluvial events, much like those seen throughout the sediment sequence at Nyayanga. Similar flows are found at other hominin sites on the Homa Peninsula (including Kanjera South), acting to bury and preserve the underlying sediments (Ditchfield et al., 2019; Stanistreet et al., 2018), an essential factor in determining whether records of hominin activity are *in situ*. Across an alluvial plain, erosion or aggradation is usually confined to small active sectors. During periods of inactivity, aeolian deposition and fluvial runoff often occur, along with pedogenic development, as observed in the sediments at Nyayanga. Moreover, lower energy unconfined fluvial activity identified at Nyayanga may be attributable to fluvial runoff as a secondary process.

5.2. Local climatic reconstruction

Based on our phytolith reconstructions, oxygen isotope studies of fossil mammals (reported here and elsewhere), and the presence of animals with aquatic habitats, such as hippopotamids, turtles, crocodilians, and cane rats (Plummer et al., 2023), the climatic conditions at Nyayanga (unit NY-1) can be characterised as moderately seasonal and well-watered. The proportion of C_3 woody vegetation is low but consistent throughout the landscape sequence. A high proportion of C_4 grasses and the generalist component of phytolith assemblages indicate consistent and dense ground cover and, further supported by the carbon isotopic composition of pedogenic carbonates, a local environment characterized as grassy woodland/bushland/shrubland. The presence of C_3 browsing taxa, such as *Deinotherium*, rhinocerotids, giraffids, a papionin monkey, and a colobine monkey, along with a minority of bovids (mostly tragelaphins), is consistent with the local abundance of woody and herbaceous C_3 plants indicated in GT7 and GT9. The low frequency of woody phytoliths at Nyayanga may be related to erosion processes and a lack of support for steady soil development, which is necessary for wooded vegetation cover. However, the low frequency of wood may also be related to phytolith production rates. Wooded vegetation produces lower amounts of phytoliths than that of grasses and herbaceous vegetation, causing them to become underrepresented in the phytolith distribution (Piperno, 2014; Mercader et al., 2009; Barboni et al., 1999).

Archaeological evidence at Nyayanga suggests that hominins utilised the area for tool production and use, including plant and animal processing. The availability of woody plant resources, such as shade, shelter, raw materials, and food, may have contributed to the attraction of hominins to the area, alongside the presence of a freshwater spring and landscape stability (Plummer et al., 2023). Hominin activities in a sparsely woody but dense grassy habitat at Nyayanga is consistent with pedogenic carbonate-based woody cover estimates at various other Early Stone Age lithic sites in the Awash, Turkana, and Olduvai basins, which also had similar mosaic habitats (Quinn et al., 2013; Finestone et al., 2024; Plummer et al., 2023). However, determining the use and, especially, the preference for certain habitat types by hominins is challenging, particularly given the uncertainty in their distribution and use of areas beyond where archaeological sites and pedogenic carbonates are forming (Negash et al., 2024). At Nyayanga, the dominance of C_4-grazing diets among many large mammalian herbivore taxa, as well as *Paranthropus* itself, underscores the significant role of grasses in the

local and surrounding landscape, as well as in the diets of at least some hominins present in the area (Plummer et al., 2023). Additionally, the significant elevational changes on the side of Mt Homa (600 m of elevation change across 5 km) would have provided a large number of habitats over short distances. The precise foods consumed by Nyayanga *Paranthropus* may have included C_4 grasses and sedges, as well as animals that consumed C_4 plants, such as butchered taxa like hippopotamids.

Both isotopic-based woody cover estimates and phytolith analysis for NY-2 indicate an increasingly open landscape, compared to the signal from NY-1, that is eventually characterised by open grasslands at NY-3 that resemble conditions at other Early Pleistocene lithic sites on the Homa Peninsula, such as Kanjera South and Sare-Abururu (Finestone et al., 2024). Carbon isotope analyses of large mammals from NY-2 to NY-3 will be important for understanding how mammal diets responded to increasingly grass-dominated landscapes.

5.3. Drivers of palaeoenvironmental change

Much like other alluvial environments, the palaeoenvironmental evolution at Nyayanga was driven by an interplay of factors. Regional and local tectonics will have had one of the most significant impacts on environmental change. The Homa Mountain carbonatite complex creates substantial changes in relief from the east to the west of Nyayanga, whilst the development of the East African Rift System created depositional lows and basins suitable for lake formation to the west of the locality, amplifying the relief of Homa Mountain through uplift (Le Bas, 1977). The location of Nyayanga on the slopes at the foot of Homa Mountain meant that sediments prograded towards the expansive depositional low to the west. Furthermore, the development and destruction of palaeolakes through faulting to the west would have led to changes in base level, which may have ultimately dictated periods of site-wide incision or deposition. Local faulting throughout the Homa Peninsula may have also led to changes in sediment supply over time through the breakdown of sediment. Drainage was likely also affected by faulting, potentially causing variations in the active sector of the alluvial plain upon which Nyayanga was located, with river capture also a possibility.

Climate and local hydrology would have been significant drivers of change at Nyayanga, affecting environmental conditions and vegetation structure. Within an alluvial plain setting, climatic changes drive the abundance of sediment supply, the release of sediment throughout the catchment, and the abundance and composition of vegetation cover, which stabilises sediment. Precipitation largely drives sediment supply to alluvial plains, with periods of higher precipitation increasing the sediment supply (Blair and McPherson, 1994b; Pope and Wilkinson, 2005). Additionally, more significant amounts of precipitation can result in higher sediment entrainment capacities, particularly in higher-magnitude episodic events (Mather and Hartley, 2005). Moister climates can often also attest to increased vegetation cover, which stabilises sediments, leading to a reduction in sediment supply (Harvey et al., 2005; Maher et al., 2007).

The sediments at Nyayanga, notably in unit NY-1, indicate a variable climate regime. Here, hyperconcentrated flows werea result of episodic high-magnitude precipitation periods, leading to an increased sediment supply due to erosion, as well as higher sediment entrainment capacities. Isotopic and phytolith evidence suggest a significant grass component to the local environment, with high levels of sediment instability. As flows moved west from Homa Mountain, they became more viscous and sediment-laden, causing them to become hyperconcentrated. Upon reaching the gentler relief of the alluvial plain at Nyayanga, these flows decelerated and aggraded across the site, particularly in the low area to the northwest. Periods of unconfined fluvial activity and fluvial runoff may have resulted from frequent precipitation, leading to more water-laden flows capable of erosion and incision, rather than significant episodic events (de Haas et al., 2014). Throughout deposition at Nyayanga, temporary periods of landscape stability and flow hiatuses become more common with time, and the environment was characterised by grassy woodland, bushland, and shrubland during NY-1, with wooded grasslands being the dominant vegetation type in NY-2 and NY-4. Progressive aridification at Nyayanga during the deposition of NY-1 to NY-3 may explain the increasing abundance of grasslands (Tipple and Pagani, 2007). Fluvial flows like those observed throughout these units, rather than hyperconcentrated flows, are often more characteristic of such climates in alluvial plains. The oxygen isotope composition of pedogenic carbonates shows no significant change through the Nyayanga sequence, however, indicating relative stasis in rainfall amount and/or moisture source and highlighting the possibility that factors other than rainfall change might play an important role in driving changes in the abundance of grasses through the Nyayanga sequence (Polissar et al., 2021; Blumenthal et al., 2017). Further oxygen isotope analyses of mammals would provide additional insight into the history of climatic change on the Homa Peninsula.

Whilst environmental conditions at Nyayanga were likely affected by variability in orbital forcing patterns, our study does not elucidate such information. Sediments at the locality appear to record a response to a local climate and environmental signal and tectonic activity. However, it is possible that precession cycles influenced moisture availability and seasonality during the deposition and erosion of the Nyayanga sediments, which may partially explain the intermittent nature of flows and their periodic hiatuses.

6. Conclusion

At Nyayanga, three sedimentary units are described, designated as NY-1 to NY-3. An alluvial plain environment was identified for the depositional environment 2.6 - 3.0 Ma (NY-1). Initial deposition occurred via episodic hyperconcentrated flows capable of mobilising cobble-grade sediment, burying underlying sediments rather than eroding them. Flow hiatuses were characterised by secondary processes including fluvial runoff and aeolian deposition, as well as pedogenic development. Throughout time, higher energy hyperconcentrated flows became absent.

Pedogenic development and deposition by secondary processes increased in frequency through the sequence. By NY-3 the landscape was relatively more stable, with soil development becoming more mature. These changes were likely caused by a migration of the active sector of the alluvial plain, although aridification may also have contributed to the reduction in the frequency of flows.

Based on published studies of fossil mammals alongside our phytolith reconstructions and oxygen isotopes, climatic conditions at Nyayanga are characterized as moderately seasonal and well-watered. Isotopic and phytolith analyses concur that the landscape remained open, with palaeovegetation fluctuating between bushy grasslands and grassy bushlands with infrequent woodland and sedges. Although there is evidence of minor variability in the local environment through the time range sampled in this study, hominin activity is evidenced throughout the sequence, suggesting that Oldowan behavioural flexibility enabled hominins to consistently exploit the locally available resources. The responses of hominins and other mammals to environmental change across the Pliocene-Pleistocene boundary at Nyayanga and other sites on the Homa Peninsula will be a focus of future research.

Declaration of competing interest

The authors declare the following financial interests/personal relationships which may be considered as potential competing interests: Thomas Plummer reports financial support was provided by National Science Foundation. Emma Finestone reports financial support was provided by National Science Foundation. Richard Potts reports

financial support was provided by William H Donner Foundation. Richard Potts reports financial support was provided by Smithsonian Institution. Thomas Plummer reports financial support was provided by Leakey Foundation. Thomas Plummer reports financial support was provided by Wenner-Gren Foundation. Scott Blumenthal reports financial support was provided by British Academy. If there are other authors, they declare that they have no known competing financial interests or personal relationships that could have appeared to influence the work reported in this paper.

7. Acknowledgements

We thank the National Museums of Kenya and E. Ndiema and F. K. Manthi (NMK Department of Earth Sciences) for support and the National Commission for Science, Technology and Innovation (NACOSTI) permits NACOSTI/P14/7709/701 and P/25/4174819 for permission. We acknowledge funding from National Science Foundation grants to TP (1327047, 2414944) and EMF (2414945) and a Graduate Research Fellowship to JW, and the William H. Donner Foundation and Smithsonian Peter Buck Fund for Human Origins Research to RP. TP also gratefully acknowledges funding from the L.S.B. Leakey Foundation (award 35805), the National Science Foundation (award 1327047), the Wenner-Gren Foundation (award 9428), and the Professional Staff Congress City University of New York Research Award Program (award 60589-0048). LCB acknowledges support from UNNC research funding. SAB acknowledges support from the British Academy (NF151155) and the University of Oregon. We acknowledge the assistance of the Palynology and Paleobotany Lab, Earth Sciences Department, National Museums of Kenya for phytolith analyses. Homa Peninsula research is conducted under the Smithsonian-National Museums of Kenya collaborative research and training agreement.

Finally, we would like to thank the two reviewers for thorough, constructive feedback that improved the paper. The editor is thanked for their patience and flexibility while the corresponding was on parental leave.

Appendix A. Supplementary data

Supplementary data to this article can be found online at https://doi.org/10.1016/j.quascirev.2026.110288.

Data availability

All data and/or code is contained within the submission.

References

Albert, R.M., Bamford, M.K., Cabanes, D., 2006. Taphonomy of phytoliths and macroplants in different soils from Olduvai Gorge (Tanzania) and the application to Plio-Pleistocene palaeoanthropological samples. Quat. Int. 148, 78–94.

Albert, R.M., Bamford, M.K., Stanistreet, I., Stollhofen, H., Rivera-Rondón, C., Rodríguez-Cintas, A., 2015. Vegetation landscape at DK locality, Olduvai Gorge, Tanzania. Palaeogeogr. Palaeoclimatol. Palaeoecol. 426, 34–45.

Albert, R.M., Ruíz, J.A., Sans, A., 2016. PhytCore ODB: a new tool to improve efficiency in the management and exchange of information on phytoliths. J. Archaeol. Sci. 68, 98–105.

Albert, R.M., Weiner, S., 2001. Study of phytoliths in prehistoric ash layers from Kebara and Tabun caves using a quantitative approach. Phytoliths: applications in earth sciences and human history 251–266.

Ashley, G.M., Tactikos, J.C., Owen, R.B., 2009. Hominin use of springs and wetlands: Paleoclimate and archaeological records from Olduvai Gorge (~ 1.79–1.74 Ma). Palaeogeogr. Palaeoclimatol. Palaeoecol. 272, 1–16.

Bamford, M.K., Albert, R.M., Cabanes, D., 2006. Plio–Pleistocene macroplant fossil remains and phytoliths from Lowermost Bed II in the eastern palaeolake margin of Olduvai Gorge, Tanzania. Quat. Int. 148, 95–112.

Barboni, D., Bonnefille, R., Alexandre, A., Meunier, J.-D., 1999. Phytoliths as paleoenvironmental indicators, west side Middle Awash Valley, Ethiopia. Palaeogeogr. Palaeoclimatol. Palaeoecol. 152, 87–100.

Behrensmeyer, A.K., Potts, R., Plummer, T., Tauxe, L., Opdyke, N., Jorstad, T., 1995. The Pleistocene locality of kanjera, Western Kenya: stratigraphy, chronology and paleoenvironments. J. Hum. Evol. 29, 247–274.

Behrensmeyer, A.K., Todd, N.E., Potts, R., Mcbrinn, G.E., 1997. Late Pliocene faunal turnover in the Turkana Basin, Kenya and Ethiopia. Science 278, 1589–1594.

Bishop, L.C., Plummer, T.W., Braun, D.R., Ditchfield, P.W., Early, E.G., Hertel, F., Lemorini, C., Oliver, J.S., Potts, R., Vincent, T., 2022. Fauna and Paleoenvironments of the Homa peninsula, Western Kenya.

Bishop, L.C., Plummer, T.W., Ferraro, J.V., Braun, D., Ditchfield, P.W., Hertel, F., Kingston, J.D., Hicks, J., Potts, R., 2006. Recent research into oldowan hominin activities at Kanjera South, Western Kenya. Afr. Archaeol. Rev. 23, 31–40.

Blair, T.C., Mcpherson, J.G., 1994a. Alluvial fan processes and forms. Geomorphology of Desert Environments. Springer.

Blair, T.C., Mcpherson, J.G., 1994b. Alluvial fans and their natural distinction from rivers based on morphology, hydraulic processes, sedimentary processes, and facies assemblages. J. Sediment. Res. 64, 450–489.

Blott, S.J., Croft, D.J., Pye, K., Saye, S.E., Wilson, H.E., 2004. Particle Size Analysis by Laser Diffraction, vol. 232. Geological Society, London, Special Publications, pp. 63–73.

Blott, S.J., Pye, K., 2001. GRADISTAT: a grain size distribution and statistics package for the analysis of unconsolidated sediments. Earth Surf. Process. Landf. 26, 1237–1248.

Blumenthal, S.A., Cerling, T.E., Chritz, K.L., Bromage, T.G., Kozdon, R., Valley, J.W., 2014. Stable isotope time-series in mammalian teeth: in situ δ18O from the innermost enamel layer. Geochem. Cosmochim. Acta 124, 223–236.

Blumenthal, S.A., Cerling, T.E., Smiley, T.M., Badgley, C.E., Plummer, T.W., 2019. Isotopic records of climate seasonality in equid teeth. Geochem. Cosmochim. Acta 260, 329–348.

Blumenthal, S.A., Levin, N.E., Brown, F.H., Brugal, J.-P., Chritz, K.L., Harris, J.M., Jehle, G.E., Cerling, T.E., 2017. Aridity and Hominin Environments, vol 114. Proceedings of the National Academy of Sciences, pp. 7331–7336.

Braun, D.R., Aldeias, V., Archer, W., Arrowsmith, J.R., Baraki, N., Campisano, C.J., Deino, A.L., Dimaggio, E.N., Dupont-Nivet, G., Engda, B., 2019. Earliest known Oldowan artifacts at> 2.58 Ma from Ledi-Geraru, Ethiopia, highlight early technological diversity. Proc. Natl. Acad. Sci. 116, 11712–11717.

Braun, D.R., Palcu Rolier, D.V., Advokaat, E.L., Archer, W., Baraki, N.G., Biernat, M.D., Beaudoin, E., Behrensmeyer, A.K., Bobe, R., Elmes, K., 2025. Early Oldowan technology thrived during Pliocene environmental change in the Turkana Basin, Kenya. Nat. Commun. 16, 9401.

Braun, D.R., Plummer, T., Ditchfield, P., Ferraro, J.V., Maina, D., Bishop, L.C., Potts, R., 2008. Oldowan behavior and raw material transport: perspectives from the Kanjera Formation. J. Archaeol. Sci. 35, 2329–2345.

Braun, H.A., 2009. Interdisciplinary Approaches to the Oldowan. Springer Netherlands, Dordrecht.

Briatico, G., Mussi, M., Melis, R.T., Geraads, D., Bocherens, H., 2024. Intra-tooth isotopic analysis shows seasonal variability in the high-elevation context of Melka Kunture (Upper Awash Valley, Ethiopia) during the early Pleistocene. Palaeogeogr. Palaeoclimatol. Palaeoecol. 655, 112555.

Brown, D.A., 1984. Prospects and limits of a phytolith key for grasses in the central United States. J. Archaeol. Sci. 11, 345–368.

Bryant, J.D., Froelich, P.N., 1995. A model of oxygen isotope fractionation in body water of large mammals. Geochem. Cosmochim. Acta 59, 4523–4537.

Bryant, J.D., Luz, B., Froelich, P.N., 1994. Oxygen isotopic composition of fossil horse tooth phosphate as a record of continental paleoclimate. Palaeogeogr. Palaeoclimatol. Palaeoecol. 107, 303–316.

Cerling, T.E., 1984. The stable isotopic composition of modern soil carbonate and its relationship to climate. Earth Planet Sci. Lett. 71, 229–240.

Cerling, T.E., Manthi, F.K., Mbua, E.N., Leakey, L.N., Leakey, M.G., Leakey, R.E., Brown, F.H., Grine, F.E., Hart, J.A., Kaleme, P., Roche, H., Uno, K.T., Wood, B.A., 2013. Stable isotope-based diet reconstructions of Turkana Basin hominins. Proc. Natl. Acad. Sci. 110, 10501–10506.

Cerling, T.E., Quade, J., Wang, Y., Bowman, J., 1989. Carbon isotopes in soils and palaeosols as ecology and palaeoecology indicators. Nature 341, 138–139.

Cerling, T.E., Wynn, J.G., Andanje, S.A., Bird, M.I., Korir, D.K., Levin, N.E., Mace, W., Macharia, A.N., Quade, J., Remien, C.H., 2011. Woody cover and hominin environments in the past 6 million years. Nature 476, 51–56.

Cohen, A.S., Campisano, C.J., Arrowsmith, J.R., Asrat, A., Beck, C.C., Behrensmeyer, A. K., Deino, A.L., Feibel, C.S., Foerster, V., Kingston, J.D., Lamb, H.F., Lowenstein, T. K., Lupien, R.L., Muiruri, V., Olago, D.O., Owen, R.B., Potts, R., Russell, J.M., Schaebitz, F., Stone, J.R., Trauth, M.H., Yost, C.L., 2022. Reconstructing the environmental context of human origins in Eastern Africa through scientific drilling. Annu. Rev. Earth Planet Sci. 50, 451–476.

de Haas, T., Ventra, D., Carbonneau, P.E., Kleinhans, M.G., 2014. Debris-flow dominance of alluvial fans masked by runoff reworking and weathering. Geomorphology 217, 165–181.

Dietze, E., Dietze, M., 2019. Grain-size distribution unmixing using the R package EMMAgeo. E&G Quaternary Science Journal 68, 29–46.

Ditchfield, P., Hicks, J., Plummer, T., Bishop, L.C., Potts, R., 1999. Current research on the Late Pliocene and Pleistocene deposits north of Homa Mountain, southwestern Kenya. J. Hum. Evol. 36, 123–150.

Ditchfield, P.W., Whitfield, E., Vincent, T., Plummer, T., Braun, D., Deino, A., Hertel, F., Oliver, J.S., Louys, J., Bishop, L.C., 2019. Geochronology and physical context of Oldowan site formation at Kanjera South, Kenya. Geol. Mag. 156, 1190–1200.

Faith, J.T., Rowan, J., Du, A., 2019. Early Hominins Evolved Within Non-analog Ecosystems, vol 116. Proceedings of the National Academy of Sciences, pp. 21478–21483.

Feibel, C.S., Brown, F.H., 1991. Age of the primate-bearing deposits on Maboko Island, Kenya. J. Hum. Evol. 21, 221–225.

Ferraro, J.V., Plummer, T.W., Pobiner, B.L., Oliver, J.S., Bishop, L.C., Braun, D.R., Ditchfield, P.W., Seaman III, J.W., Binetti, K.M., Seaman, J.R.J.W., 2013. Earliest archaeological evidence of persistent hominin carnivory. PLoS One 8, e62174.
Finestone, E.M., Plummer, T.W., Ditchfield, P.W., Reeves, J.S., Braun, D.R., Bartilol, S.K., Rotich, N.K., Bishop, L.C., Oliver, J.S., Kinyanjui, R.N., 2025. Selective use of distant stone resources by the earliest Oldowan toolmakers. Sci. Adv. 11, eadu5838.
Finestone, E.M., Plummer, T.W., Vincent, T.H., Blumenthal, S.A., Ditchfield, P.W., Bishop, L.C., Oliver, J.S., Herries, A.I., Palfery, C.V., Lane, T.P., 2024. New Oldowan locality Sare-Abururu (ca. 1.7 Ma) provides evidence of diverse hominin behaviors on the Homa Peninsula, Kenya. J. Hum. Evol. 190, 103498.
Folk, R.L., Ward, W.C., 1957. Brazos river bar; a study in the significance of grain size parameters. J. Sediment. Petrol. 27, 3–26.
Fricke, H.C., Clyde, W.C., O'Neil, J.R., 1998. Intra-tooth variations in δ18O (PO4) of mammalian tooth enamel as a record of seasonal variations in continental climate variables. Geochem. Cosmochim. Acta 62, 1839–1850.
Gray, A.B., Pasternack, G.B., Watson, E.B., 2010. Hydrogen peroxide treatment effects on the particle size distribution of alluvial and marsh sediments. Holocene 20, 293–301.
Green, D.R., Smith, T.M., Green, G.M., Bidlack, F.B., Tafforeau, P., Colman, A.S., 2018. Quantitative reconstruction of seasonality from stable isotopes in teeth. Geochem. Cosmochim. Acta 235, 483–504.
Harmand, S., Lewis, J.E., Feibel, C.S., Lepre, C.J., Prat, S., Lenoble, A., Boës, X., Quinn, R. L., Brenet, M., Arroyo, A., 2015. 3.3-million-year-old stone tools from Lomekwi 3, West Turkana, Kenya. Nature 521, 310–315.
Harvey, A.M., Mather, A.E., Stokes, M., 2005. Alluvial Fans: Geomorphology, Sedimentology, dynamics–introduction. A Review of alluvial-fan Research. Geological Society of London, London.
Hay, R., Kyser, T., 2001. Chemical sedimentology and paleoenvironmental history of Lake Olduvai, a Pliocene lake in northern Tanzania. Geol. Soc. Am. Bull. 113, 1505–1521.
Hoppe, K.A., 2006. Correlation between the oxygen isotope ratio of North American bison teeth and local waters: implication for paleoclimatic reconstructions. Earth Planet Sci. Lett. 244, 408–417.
Huertas, A.D., Iacumin, P., Stenni, B., Chillón, B.S., Longinelli, A., 1995. Oxygen isotope variations of phosphate in mammalian bone and tooth enamel. Geochem. Cosmochim. Acta 59, 4299–4305.
Kent, P.E., 1942. The Pleistocene beds of Kanam and Kanjera, Kavirondo, Kenya. Geol. Mag. 79, 117–132.
Kinyanjui, R., 2012. Phytolith Analysis as a Palaeoecological Tool for Reconstructing Mid-to Late-Pleistocene Environments in the Olorgesailie Basin, Kenya.
Kohn, M.J., 1996. Predicting animal δ18O: accounting for diet and physiological adaptation. Geochem. Cosmochim. Acta 60, 4811–4829.
Kohn, M.J., Schoeninger, M.J., Valley, J.W., 1998. Variability in oxygen isotope compositions of herbivore teeth: reflections of seasonality or developmental physiology? Chem. Geol. 152, 97–112.
Konert, M., Vandenberghe, J., 1997. Comparison of laser grain size analysis with pipette and sieve analysis: a solution for the underestimation of the clay fraction. Sedimentology 44, 523–535.
Kusaka, S., Nakano, T., 2014. Carbon and oxygen isotope ratios and their temperature dependence in carbonate and tooth enamel using a GasBench II preparation device: letter to the editor. Rapid Commun. Mass Spectrom. 28, 563–567.
Le Bas, M.J., 1977. Carbonatite-Nephelinite Volcanism: an African Case History. John Wiley and Sons, New York.
Levin, N.E., Brown, F.H., Behrensmeyer, A.K., Bobe, R., Cerling, T.E., 2011. Paleosol carbonates from the Omo Group: isotopic records of local and regional environmental change in East Africa. Palaeogeogr. Palaeoclimatol. Palaeoecol. 307, 75–89.
Liu, B., Qu, J., Ning, D., Gao, Y., Zu, R., An, Z., 2014. Grain-size study of aeolian sediments found east of Kumtagh Desert. Aeolian Res. 13, 1–6.
Longinelli, A., 1984. Oxygen isotopes in mammal bone phosphate: a new tool for paleohydrological and paleoclimatological research? Geochem. Cosmochim. Acta 48, 385–390.
Lupien, R.L., Russell, J.M., Yost, C.L., Kingston, J.D., Deino, A.L., Logan, J., Schuh, A., Cohen, A.S., 2021. Vegetation change in the Baringo Basin, East Africa across the onset of Northern Hemisphere glaciation 3.3–2.6 Ma. Palaeogeogr. Palaeoclimatol. Palaeoecol. 570, 109426.
Machette, M.N., 1985. Calcic Soils of the Southwestern United States, vol 203. Geological Society of America.
Madella, M., Alexandre, A., Ball, T., 2005. International code for phytolith nomenclature 1.0. Ann. Bot. 96, 253–260.
Maher, E., Harvey, A.M., France, D., 2007. The impact of a major Quaternary river capture on the alluvial sediments of a beheaded river system, the Rio Alias SE Spain. Geomorphology 84, 344–356.
Maslin, M.A., Brierley, C.M., Milner, A.M., Shultz, S., Trauth, M.H., Wilson, K.E., 2014. East African climate pulses and early human evolution. Quat. Sci. Rev. 101, 1–17.
Mather, A., Stokes, M., Whitfield, E., 2017. River terraces and alluvial fans: the case for an integrated Quaternary fluvial archive. Quat. Sci. Rev. 166, 74–90.
Mather, A.E., Hartley, A., 2005. Flow Events on a hyper-arid Alluvial Fan: Quebrada Tambores, Salar De Atacama, Northern Chile.
Mclaren, P., Bowles, D., 1985. The effects of sediment transport on grain-size distributions. J. Sediment. Res. 55, 457–470.
Mercader, J., Akuku, P., Boivin, N., Bugumba, R., Bushozi, P., Camacho, A., Carter, T., Clarke, S., Cueva-Temprana, A., Durkin, P., 2021. Earliest Olduvai hominins exploited unstable environments~ 2 million years ago. Nat. Commun. 12, 3.
Mercader, J., Bennett, T., Esselmont, C., Simpson, S., Walde, D., 2009. Phytoliths in woody plants from the miombo woodlands of Mozambique. Ann. Bot. 104, 91–113.
Meyer, I., Davies, G.R., Vogt, C., Kuhlmann, H., Stuut, J.-B.W., 2013. Changing rainfall patterns in NW Africa since the Younger Dryas. Aeolian Res. 10, 111–123.
Miall, A.D., 2013. The Geology of Fluvial Deposits: Sedimentary Facies, Basin Analysis, and Petroleum Geology. Springer.
Mutai, C.C., Ward, M.N., 2000. East African rainfall and the tropical circulation/convection on intraseasonal to interannual timescales. J. Clim. 13, 3915–3939.
Negash, E.W., Alemseged, Z., Barr, W.A., Behrensmeyer, A.K., Blumenthal, S.A., Bobe, R., Carvalho, S., Cerling, T.E., Chritz, K.L., Mcguire, E., 2024. Modern African ecosystems as landscape-scale analogues for reconstructing woody cover and early hominin environments. J. Hum. Evol. 197, 103604.
Neumann, K., Strömberg, C.A., Ball, T., Albert, R.M., Vrydaghs, L., Cummings, L.S., 2019. International code for phytolith nomenclature (ICPN) 2.0. Ann. Bot. 124, 189–199.
North, C.P., Davidson, S.K., 2012. Unconfined alluvial flow processes: recognition and interpretation of their deposits, and the significance for palaeogeographic reconstruction. Earth Sci. Rev. 111, 199–223.
Norwood, A.L., Rowan, J., Faith, J.T., 2025. Reconciling the environmental implications of late Quaternary faunal and pollen records in southern Africa. Quaternary Science Advances 17, 100259.
Oliver, J.S., Plummer, T.W., Hertel, F., Bishop, L.C., 2019. Bovid mortality patterns from Kanjera South, Homa Peninsula, Kenya and FLK-Zinj, Olduvai Gorge, Tanzania: evidence for habitat mediated variability in Oldowan hominin hunting and scavenging behavior. J. Hum. Evol. 131, 61–75.
Passey, B.H., Cerling, T.E., 2002. Tooth enamel mineralization in ungulates: implications for recovering a primary isotopic time-series. Geochem. Cosmochim. Acta 66, 3225–3234.
Paterson, G.A., Heslop, D., 2015. New methods for unmixing sediment grain size data. G-cubed 16, 4494–4506.
Patterson, D., Braun, D., Behrensmeyer, A.K., Merritt, S., Zliobaite, I., Reeves, J., Wood, B., Fortelius, M., Bobe, R., 2017. Ecosystem evolution and hominin paleobiology at East Turkana, northern Kenya between 2.0 and 1.4 Ma. Palaeogeogr. Palaeoclimatol. Palaeoecol. 481, 1–13.
Pickford, M., 1982. The tectonics, volcanics and sediments of the Nyanza Rift Valley, Kenya. Zeitschrift für Geomorphologie. Supplementband Stuttgart 1–33.
Pickford, M., 1984. Kenya Palaeontology Gazetteer: Western Kenya. National Museums of Kenya, Department of Sites and Monuments Documentation.
Pierson, T.C., 2005. Distinguishing between debris flows and floods from field evidence in small watersheds, USGS Fact Sheet 2004-3142. US Geological Survey.
Piperno, D.R., 2006. Phytoliths: a Comprehensive Guide for Archaeologists and Paleoecologists. Rowman Altamira.
Piperno, D.R., 2014. Phytolyth Analysis: an Archaeological and Geological Perspective. Elsevier.
Piperno, D.R., Pearsall, D.M., 1998. The silica bodies of tropical American grasses: morphology, taxonomy, and implications for grass systematics and fossil phytolith identification. Smithsonian Contrib. Bot.
Plummer, T., Bishop, L.C., Ditchfield, P., Hicks, J., 1999. Research on Late Pliocene oldowan sites at kanjera south, Kenya. J. Hum. Evol. 36, 151–170.
Plummer, T.W., Bishop, L.C., 1994. Hominid paleoecology at Olduvai Gorge, Tanzania as indicated by antelope remains. J. Hum. Evol. 27, 47–75.
Plummer, T.W., Bishop, L.C., 2016. Oldowan hominin behavior and ecology at Kanjera South, Kenya. Journal of Anthropological Sciences 94.
Plummer, T.W., Ditchfield, P.W., Bishop, L.C., Kingston, J.D., Ferraro, J.V., Braun, D.R., Hertel, F., Potts, R., 2009. Oldest evidence of toolmaking hominins in a grassland-dominated ecosystem. PLoS One 4, e7199.
Plummer, T.W., Harmand, S., Finestone, E.M., Wilson, E.P., 2025. The first million years of technology: the lomekwian and the early oldowan. Annu. Rev. Anthropol. 54.
Plummer, T.W., Oliver, J.S., Finestone, E.M., Ditchfield, P.W., Bishop, L.C., Blumenthal, S.A., Lemorini, C., Caricola, I., Bailey, S.E., Herries, A.I.R., Parkinson, J. A., Whitfield, E., Hertel, F., Kinyanjui, R.N., Vincent, T.H., Li, Y., Louys, J., Frost, S. R., Braun, D.R., Reeves, J.S., Early, E.D.G., Onyango, B., Lamela-Lopez, R., Forrest, F. L., He, H., Lane, T.P., Frouin, M., Nomade, S., Wilson, E.P., Bartilol, S.K., Rotich, N. K., Potts, R., 2023. Expanded geographic distribution and dietary strategies of the earliest Oldowan hominins and *Paranthropus*. Science 379, 561–566.
Polissar, P.J., Uno, K.T., Phelps, S.R., Karp, A.T., Freeman, K.H., Pensky, J.L., 2021. Hydrologic changes drove the late Miocene expansion of C4 grasslands on the Northern Indian subcontinent. Paleoceanogr. Paleoclimatol. 36, e2020PA004108.
Pope, R.J., Wilkinson, K.N., 2005. Reconciling the Roles of Climate and Tectonics in Late Quaternary Fan Development on the Spartan Piedmont, Greece.
Potts, R., 1994. Variables versus models of early Pleistocene hominid land use. J. Hum. Evol. 27, 7–24.
Potts, R., 2012. Evolution and environmental change in early human prehistory. Annu. Rev. Anthropol. 41, 151–167.
Potts, R., Behrensmeyer, A.K., Ditchfield, P., 1999. Paleolandscape variation and Early Pleistocene hominid activities: members 1 and 7, Olorgesailie Formation, Kenya. J. Hum. Evol. 37, 747–788.
Potts, R., Behrensmeyer, A.K., Faith, J.T., Tryon, C.A., Brooks, A.S., Yellen, J.E., Deino, A. L., Kinyanjui, R., Clark, J.B., Haradon, C.M., 2018. Environmental dynamics during the onset of the Middle Stone Age in eastern Africa. Science 360, 86–90.
Quinn, R.L., Lepre, C.J., Feibel, C.S., Wright, J.D., Mortlock, R.A., Harmand, S., Brugal, J.-P., Roche, H., 2013. Pedogenic carbonate stable isotopic evidence for wooded habitat preference of early Pleistocene tool makers in the Turkana Basin. J. Hum. Evol. 65, 65–78.
Retallack, G.J., 2005. Pedogenic carbonate proxies for amount and seasonality of precipitation in paleosols. Geology 33, 333–336.
Saggerson, E.P., 1952. Geology of the Kisumu District. Geological Survey of Kenya.
Ségalen, L., Lee-Thorp, J.A., Cerling, T., 2007. Timing of C4 grass expansion across Sub-Saharan Africa. J. Hum. Evol. 53, 549–559.

Semaw, S., Renne, P., Harris, J.W., Feibel, C.S., Bernor, R.L., Fesseha, N., Mowbray, K., 1997. 2.5-million-year-old stone tools from Gona, Ethiopia. Nature 385, 333–336.
Sharp, Z., Cerling, T., 1998. Fossil isotope records of seasonal climate and ecology: straight from the horse's mouth. Geology 26, 219–222.
Sikes, N.E., 1994. Early hominid habitat preferences in East Africa: paleosol carbon isotopic evidence. J. Hum. Evol. 27, 25–45.
Souron, A., Balasse, M., Boisserie, J.-R., 2012. Intra-tooth isotopic profiles of canines from extant Hippopotamus amphibius and late Pliocene hippopotamids (Shungura Formation, Ethiopia): insights into the seasonality of diet and climate. Palaeogeogr. Palaeoclimatol. Palaeoecol. 342, 97–110.
Stanistreet, I.G., Mchenry, L.J., Stollhofen, H., De La Torre, I., 2018. Bed II Sequence Stratigraphic context of EF-HR and HWK EE archaeological sites, and the Oldowan/Acheulean succession at Olduvai Gorge, Tanzania. J. Hum. Evol. 120, 19–31.
Tipple, B.J., Pagani, M., 2007. The early origins of terrestrial C4 photosynthesis. Annu. Rev. Earth Planet Sci. 35, 435–461.
Toth, N., Schick, K., 2018. An overview of the cognitive implications of the Oldowan Industrial Complex. Azania 53, 3–39.
Twiss, P.C., Suess, E., Smith, R.M., 1969. Morphological classification of grass phytoliths. Soil Sci. Soc. Am. J. 33, 109–115.
Uno, K.T., Polissar, P.J., Jackson, K.E., Demenocal, P.B., 2016a. Neogene Biomarker Record of Vegetation Change in Eastern Africa, vol 113. Proceedings of the National Academy of Sciences, pp. 6355–6363.
Uno, K.T., Polissar, P.J., Kahle, E., Feibel, C., Harmand, S., Roche, H., Demenocal, P.B., 2016b. A Pleistocene palaeovegetation record from plant wax biomarkers from the Nachukui Formation, West Turkana, Kenya. Phil. Trans. Biol. Sci. 371, 20150235.
Uno, K.T., Rivals, F., Bibi, F., Pante, M., Njau, J., De La Torre, I., 2018. Large mammal diets and paleoecology across the Oldowan–Acheulean transition at Olduvai Gorge, Tanzania from stable isotope and tooth wear analyses. J. Hum. Evol. 120, 76–91.
Uribelarrea, D., Martín-Perea, D., Díez-Martín, F., Sánchez-Yustos, P., Dominguez-Rodrigo, M., Baquedano, E., Mabulla, A., 2017. A reconstruction of the paleolandscape during the earliest Acheulian of FLK West: the co-existence of Oldowan and Acheulian industries during lowermost Bed II (Olduvai Gorge, Tanzania). Palaeogeogr. Palaeoclimatol. Palaeoecol. 488, 50–58.
van der Bilt, W.G., Barr, I.D., Berben, S.M., Hennekam, R., Lane, T., Adamson, K., Bakke, J., 2021. Late Holocene canyon-carving floods in northern Iceland were smaller than previously reported. Commun. Earth Environ. 2, 86.
Vandenberghe, J., 2013. Grain size of fine-grained windblown sediment: a powerful proxy for process identification. Earth Sci. Rev. 121, 18–30.
Vrba, E.S., 1985. Ecological and adaptive changes associated with early hominid evolution. Ancestors: the hard evidence 63–71.
Weltje, G.J., 1997. End-member modeling of compositional data: Numerical-statistical algorithms for solving the explicit mixing problem. Math. Geol. 29, 503–549.
Weltje, G.J., Prins, M.A., 2003. Muddled or mixed? Inferring palaeoclimate from size distributions of deep-sea clastics. Sediment. Geol. 162, 39–62.
Weltje, G.J., Prins, M.A., 2007. Genetically meaningful decomposition of grain-size distributions. Sediment. Geol. 202, 409–424.
Zeller, E., Timmermann, A., Yun, K.-S., Raia, P., Stein, K., Ruan, J., 2023. Human adaptation to diverse biomes over the past 3 million years. Science 380, 604–608.